NTNU – Trondheim
Norwegian University of
Science and Technology

Optimal Operation of Wind Farms

Andre Brandal

Master of Science in Engineering Cybernetics (2)
Submission date: July 2013
Supervisor: Steinar Sælid, ITK

Norwegian University of Science and Technology
Department of Engineering Cybernetics

Summary

In this project we considered the wind farm operation planning to maximize the total power produced. The wind farm consisted of a row of three wind turbines. Two strategies were evaluated. The first strategy was to rotate the turbines wake away from the downwind turbines by the use of yaw control. The second strategy was to reduce the most upwind turbines power coefficient. The two strategies was simulated where they were first tested individually, then a combination of them was evaluated. It was concluded that both of the strategies increased the total power production individually. The yaw effect showed that it could potentially give a much larger total power production compared to the effect from the frontal turbine power coefficient reduction. The increase in power production from the yaw effect is dependent on the yaw angle[1], this increased angle will also induce larger structural loads. When a combination of the two strategies was simulated, the total power production was lower than with the yaw effect alone.

[1] This is true when the wind is constant in the prevailing direction

Sammendrag

I dette prosjektet tok vi for oss driftsplanlegging av en vindmøllepark med den hensikt i å maksimere den totale effektproduksjonen. Vindmølleparken bestod av en rekke med tre vindturbiner. To ulilke strategier ble evaluert. Den første strategien var å rotere windturbinenes kjølvann vekk fra de bakomliggende vindturbinene ved hjelp av å rotere selve vindturbinen. Den andre strategien var å redusere den fremste vindturbinens effektkoeffisient. Begge strategiene ble simulert der hver strategi ble først tested individuelt, så en kombinasjon av dem begge. Det ble konkludert at begge strategiene individuelt gav en økning i den totale effektproduksjonen. Roteringsstrategien viste seg å potensielt gi mye større total effektproduksjon sammenlignet med strategien der en reduserer den fremste vindturbinens effektkoeffisient. Økningen i effektproduksjon ved rotering er avhengig av roteringsvinkelen hvor økt vinkel gir mer effektproduksjon[2]. Problemet er at en økt roteringsvinkel også gir større belastning på vindmøllen. Da begge strategiene ble kombinert, viste det seg at roteringsstrategien var mer effektiv når den ble brukt alene.

[2]Dette stemmer så lenge vinden er konstant i den rådende vindretningen

Contents

List of Figures

Nomenclature

β	Pitch angle
λ	Tip speed ratio
Ω	Rotational velocity(rad/s)
ρ	Air density
θ	Angle between the wind direction and the direction of the rotor
C_p	Power coefficient
C_T	Thrust coefficient
D_0	The rotor diameter
D_w	The diameter of the wake
I_{amb}	Ambient turbulence
I_{total}	Total turbulence intensity
I_w	Turbulence added from the wake
V_d	Wind speed immediately behind the rotor
V_∞	Free stream wind velocity
δV	The velocity deficit
A	Rotor swept area
a	Axial induction factor
k	Wake decay constant

1 Introduction

For over hundreds of years, power has been extracted in various ways from the wind. In the 16th century, Windmills was typically being used by farmers for pumping water and grinding wheat, the same applied in the late 18th century, but now also for generating electricity. The design of the historic wind extracting machines, was typically large, inefficient and heavy, and was replaced in the 19th century by fossil fuel. Because of the improved understanding of aerodynamics and materials and the increased awareness of the negative environmental effects from fossil fuel, wind energy is now becoming more and more competitive with the more traditional energy sources. The wide use of wind energy has led to the installation of more and larger wind farms. The groupings of turbines lead to challenges from the increased wake interactions between the turbines and also extra maintenance cost due to the increased turbulence intensity.

The mutual interaction between the turbines leads to a reduction of the total power production, this is mainly because of the lower wind speeds from the wakes behind the rotor blades. To reduce the power losses, it is important to obtain a detailed understanding of the wind turbine behaviour. This is most effectively done by computer simulation. In order to properly simulate the interactions between several turbines, the study of suitable wake models are important.

Because of the integration of large amounts of wind power in the electricity grid, wind farm control and management will become an increasingly important issue. Wind turbines have and are still being treated as single units where the objective is to maximize its energy production. As the wind is fluctuating, so is the power output and frequency from the turbines, this is problematic in the sense of grid stability. It is therefore good reasons to incorporate collective control strategies such that wind farms are treated as single units where the energy output may be regulated due to the requirements from the system operators. Wind power is always fluctuating; to secure good system planning it is important to use good forecasting methods to predict future wind speeds. Short-term forecasting is usually used for the prediction of energy generation and power systems operations.

It is often of importance to optimize the wind farm to produce maximum power. Obviously, the planning process is important because an optimal layout may help maximize the energy yield and at the same time minimize the area and number of wind turbines. Operation planning is important, where different control strategies to maximize the power output are utilized. Pitch and yaw control is typically used. Pitch control is used to limit the peak power at high wind speeds, but also to maximize the energy yield at low wind speeds. Yaw control is typically used to maximize the wind energy capture by rotating the turbine such that the blades perpendicularly face the wind stream.

In this project, the available literature on important topics regarding the interaction with the energy grid, weather forecasting, control strategies and commonly used wake models are reviewed. Finally, we consider a wind farm consisting of three turbines. Two strategies are simulated where the goal is to increase the total power production of the wind farm.

The main chapters in this report are structured as follows:

Chapter 2 Gives an introduction to the fundamentals of wind power.

Chapter 3 Discuss the implications of increased wind energy in the electrical grid. Last part is about the use of different generators and frequency control.

Chapter 4 The importance of weather forecasting is discussed. Also, the types of models and derivation of different time series models commonly used for wind prediction is given.

Chapter 5 The effects from the mutual interaction between the turbines are discussed. Different wake models are then presented.

Chapter 6 The chapter starts with a presentation of a typical wind turbine controller, and then a wind farm controller is presented. The chapter ends with a discussion about operation planning to maximize the power production.

Chapter 7 Two strategies to maximize a wind farm power production are simulated; the chapter ends with a short discussion of the results.

Chapter 8 and 9 Final discussion and conclusions.

2 Wind turbines

2.1 Fundamentals of wind power

The wind power flowing through an area of interest depends on the amount of air, speed of air and its mass, wind turbines extracts the kinetic energy to generate power. The definition of kinetic energy is:

$$KE = \frac{1}{2}mv^2 \tag{1}$$

Power is energy per unit time, the power P is:

$$P_0 = \frac{1}{2}\dot{m}v^2 \tag{2}$$

We know from fluid mechanics, that $\dot{m} = \rho A v$, inserting for $\dot{m}$ we get the fundamental equation of wind power:

$$P_0 = \frac{1}{2}\rho A v^3 \tag{3}$$

where ρ is the air density, A is the rotor swept area.

2.1.1 One dimentional actuator disc theory

It is common to describe wind turbines by the use of the actuator disc concept. The wind that passes through the rotor blades(disc) loses some of its kinetic energy, and therefore slows down from the far upwind(free stream) velocity V_∞ to the average value for the downstream in the wake V_w. The speed immediately behind the disc(rotor) is V_d. As seen in figure 1, the static pressure increases from its upstream pressure p_∞ to p_d^+ just in front of the rotor disc, it then immediately drops to p_d^- behind the rotor disc which is associated to the axial force exerted by the disc. From p_d^-, the pressure gradually recovers further down the wake until it reaches back to p_∞. This actuator disc's energy extraction may be used as a black box and then use the equations of conservation of mass, momentum and energy, for incompressible flow[13].
From the continuity equation, we get:

$$\dot{m} = \rho A_\infty V_\infty = \rho A_d V_d = \rho A_w V_w \tag{4}$$

The force on the rotor disc:

$$T = \dot{m}(V_\infty - V_w) = (p_d^+ - p_d^-)A_d \tag{5}$$

and finally the extracted energy:

$$E = \frac{1}{2}m(V_\infty^2 - V_w^2) \tag{6}$$

from 2, we have the energy extracted per unit time, the power, $P = \frac{1}{2}\dot{m}(V_\infty^2 - V_w^2)$. Inserting equation 5 gives us, $P = TV_d = \dot{m}(V_\infty - V_w)V_d$. This leads to by equating the two expressions:

$$V_d = \frac{1}{2}(V_\infty + V_w) \tag{7}$$

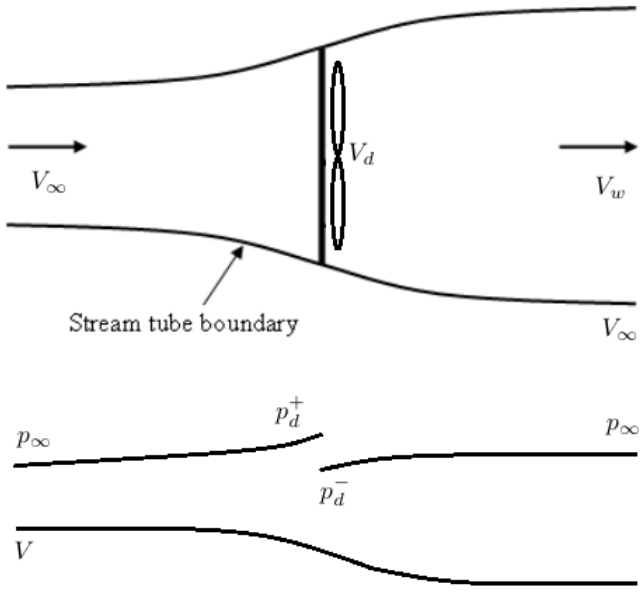

Figure 1: Pressure and wind speed through an actuator disc.

2.1.2 Efficiency in Extracting Wind Power

In order to compare the efficiency of different wind turbines we have the power coefficient, C_p, which is the ratio of the power extracted by the turbine over the total available power. By using equation the fundamental equation of wind power, we can define C_p by $P = P_0 C_p$, we then get:

$$C_p = \frac{P}{P_0} = \frac{P}{\frac{1}{2}\rho V_\infty^3 A_d} \tag{8}$$

the power is non-dimensionalized by the wind speed and the rotor swept area. We can thus expand the expression for C_p by:

$$C_p = \frac{1}{2}(V_\infty + V_w)(V_\infty^2 - V_w^2)/V_\infty^3 = \frac{1}{2}(1+b)(1-b^2) = 4a(1-a)^2 \tag{9}$$

where a is the fractional decrease in the wind velocity between the free stream and the rotor plane, called the axial induction factor. The equation for a is:

$$a = \frac{V_\infty - V_d}{V_\infty} \tag{10}$$

and b is defined as, $b = \frac{V_w}{V_\infty}$.

One may find the thrust coefficient C_T in the same way:

$$C_T = \frac{T}{\frac{1}{2}\rho V_\infty^2 A_d} = 1 - b^2 = 4a(1-a) \tag{11}$$

To summarize, we may write the power and thrust coefficient as a function of the axial induction factor as:

$$C_p = 4a(1-a)^2 \tag{12a}$$
$$C_T = 4a(1-a) \tag{12b}$$

2.1.3 The Betz limit

In 1919 the physicist Albert Betz showed that for a hypothetical wind-extraction machine, the fundamental laws of conservation of mass and energy allowed maximum $\frac{16}{27} \approx 59.3\%$ of the kinetic energy to be captured. The maximum value of C_p is therefore $59,3\%$. We can write $a = (1-b)/2$, the optimal C_p is found when $a = b = \frac{1}{3}$ such that $C_p = \frac{16}{27} \approx 0,5926$[13]. This Betz' law limit is ideal, and can therefore not be fully reached in practice, see figure 2 where the top is reached when the axial induction factor a is $\frac{1}{3}$.

The value of C_p is unique to each wind turbine and is also a function of the wind speed. As the Betz Limit is a theoretical maximum, the common values of today's best designed wind turbines operate at values of 0.35-0.45. When we consider all the other factors that come with a complete wind turbine system, only 10-30% of the wind is actually converted to usable electricity[34].

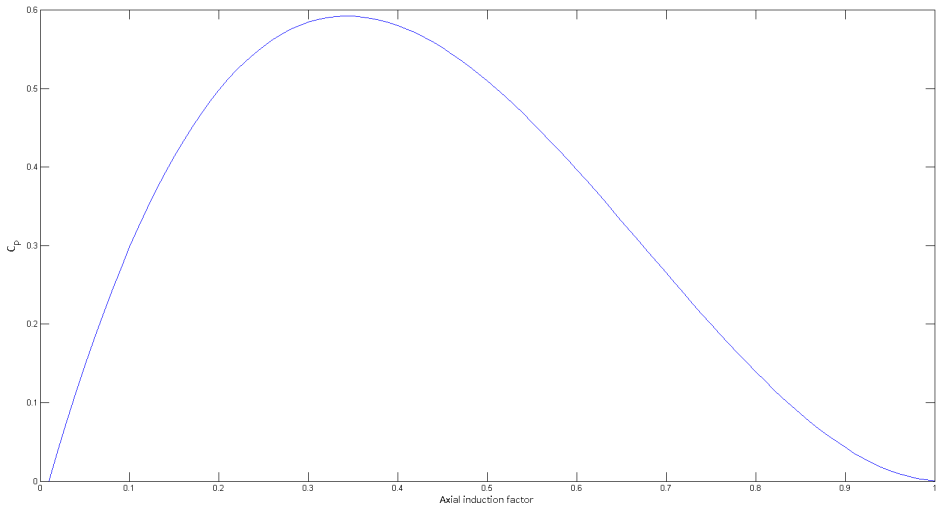

Figure 2: Power coefficient as a function of the axial induction factor

2.1.4 The tip speed ratio

The definition of the tip speed ratio is the relationship between the tangential velocity of the tip of the rotor blade velocity to the relative (free stream) wind velocity. The tip speed ratio λ is defined as:

$$\lambda = \frac{\Omega r}{V_\infty} \tag{13}$$

where Ω is the rotational velocity(rad/s), r is the rotor blade radius and V_∞ is the far upwind wind velocity. If a rotor rotates slowly compared to the wind, it allows too much wind to pass through and therefore doesn't extract the all the energy potential. On the other hand, if the rotor rotates too quickly, it appears to the wind as a large "flat disc", this creates a large amount of drag. The rotor tip speed ratio depends on the blade airfoil profile used, the number of blades, and the type of wind turbine. It is today most common with three bladed wind turbines, these typically operate at $\lambda = 6 - 8$. A wind turbine with fewer rotor blades have to rotate faster to extract the maximum power from the wind and also usually operate at a higher TSR compared to a turbine with more blades. A relatively high TSR is generally desirable since it results in a high shaft rotational speed that allows efficient operation of an electric generator[15].

The efficiency of a turbine can be increased with higher tip speeds, however, when the tip speed is high, further increase may be insignificant, specially when considering the penalties. See figure 3. A higher TSR leads to higher centrifugal and aerodynamic forces, these forces signify the challenges of maintaining structural integrity. Aerodynamics of the blade design thus play a much more critical role[14].

Tip speed ratio	Lower	Higher
Value	Tip speeds of one to two	Tip speeds higher than 10
Utilization	Traditional wind mills and water pumps	Mainly single or two bladed prototypes
Torque	Increases	Decreases
Efficiency	Decreases significantly below five due to rotational wake created by high torque	Insignificant increases after eight
Centrifugal Stress	Decreases	Increases as a square of rotational velocity
Aerodynamic Stress	Decreases	Increases proportionally with rotational velocity
Area of Solidity	Increases	Decreases significantly
Blade Profile	Large	Significantly Narrow
Aerodynamics	Simple	Critical
Noise	Increases to the 6^{th} power approximately	

Figure 3: TSR design considerations, re-drawn from[14]

2.2 Wind turbine operation

The aerodynamic conversion that occurs at the rotor is the most important part of the wind turbine operation. The force generated by the wind upon the blades may be divided into two components. The first is the rotor torque which acts in the direction of rotation, which causes the rotor torque, T_r. The second is the rotor thrust, F_T, which acts in the direction perpendicular to the rotor. The equation of the rotor torque and the rotor thrust, together with the aerodynamic power P_a which is the power input to the wind turbine, is given as:

$$P_a(t) = \frac{1}{2}\rho A_d V_\infty^3 C_p(\lambda(t), \beta(t)) \tag{14}$$

$$T_r(t) = \frac{\pi}{2}\rho R_d^3 V_\infty^2 C_Q(\lambda(t), \beta(t)) \tag{15}$$

$$F_T(t) = \frac{1}{2}\rho A_d V_\infty^2 C_T(\lambda(t), \beta(t)) \tag{16}$$

where ρ is the density of the air, the functions $C_p(\lambda(t), \beta(t))$, $C_Q(\lambda(t), \beta(t))$ and $C_T(\lambda(t), \beta(t))$ are the power, torque and thrust coefficient, written as a function of the tip speed ratio λ and the pitch angle β. The torque coefficient is given as:

$$C_Q(\lambda(t), \beta(t)) = \frac{1}{\lambda} C_p(\lambda(t), \beta(t)) \tag{17}$$

The thrust force causes oscillation of the tower due to the elasticity of the structure. It is important to reduce these; this is the task for the wind turbine controller. Bad controller design and thus amplifications of these oscillations may lead to damage to the structure.

2.3 Wind turbine structure and design

There are two main classes of wind turbines; they are classified by the orientation of the shaft and rotational axis. The two types are the horizontal axis and vertical axis wind turbines, both with several different generator types. The horizontal axis wind turbines(HAWT) has its blades rotating on an axis perpendicular to the ground where the vertical axis wind turbine(VAWT) has its axis normal to the ground.
These two types has both each favourable characteristics, however, the HAWT configuration is the type commonly used today[20]. In comparison to the HAWT's, the VAWT's is not dependent on the direction of the wind, thus, they do not need a yawing control system which help the turbine to face directly against the wind direction. This is one of the great advantages of the VAWT design compared to HAWT.
Figure 4 depicts a simplified model of the structure of a horizontal axis wind turbine. The main part of the wind turbine is the blades, nacelle and the tower. The energy is converted when the rotating blades catches the wind which then is transferred to the gearbox via the low speed shaft. From the gear box, a high speed shaft is connected to the generator from where the energy is fed to the electric grid.

Today, the energy is generated through an asynchronous generator to vary the output frequency and voltage to match the constant value of the grid. The Doubly-fed Induction Generator (DFIG) is the usual system for today's modern wind turbines. The largest wind turbines today is usually operating with rotation speeds of 15-20 rpm. Most of today's commercial wind turbines is installed with three blades, but some manufacturers only use two - or even one blade. Three bladed HAWTs generally utilize a lower tip speed ratio than those with one or two blades[15]. More blades also mean that the same amount of energy may be captured at lower rotational speeds.

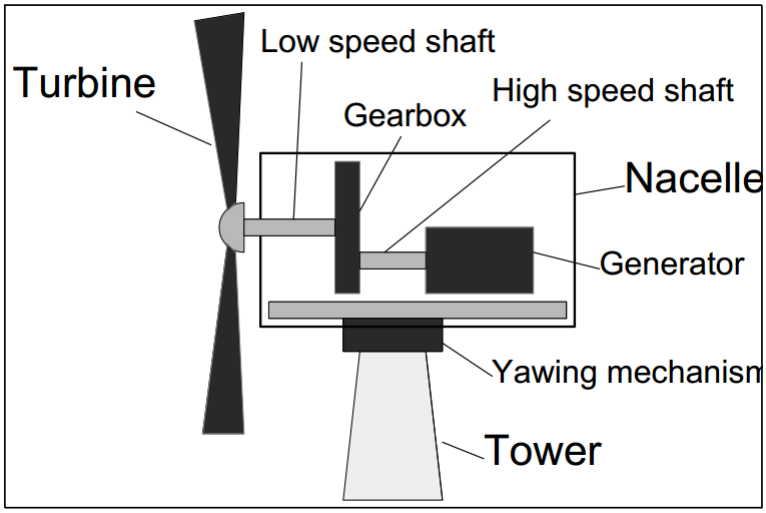

Figure 4: A simple illustration of a horizontal axis wind turbine, source [20]

2.4 Region of operation

The maximum power that can be extracted from the wind is a function of the wind speed which is the cube of the wind speed. This means that if the wind speed doubles, the power increases eight times. Due to this fact and because the wind is stronger higher above the ground due to surface friction, a small increase in hub height of the wind turbine may lead to a large increase in potential power extraction. The control mechanism of each wind turbines is usually dependent on which operating region it is in. These regions are commonly divided into region 1, 2, 3. See figure 5. Region 1 is commonly wind speeds below $5m/s$, this is where the wind doesn't have sufficient power to be useful. Region 2 starts at the minimum speed at which the turbine will generate power, in this region we want to capture as much power as possible. Region 3 is reached when the wind speed is high enough for the turbine to reach its rated power output, it is then necessary to limit the power captured to make sure that electrical and mechanical loads are limited[1].
At very high wind speeds, wind turbines shut down, this wind speed is called the "cut-out" speed. This is a safety measure to protect the turbines from damage. Electrical/mechanical brakes, pitch and yaw control may be used for this.

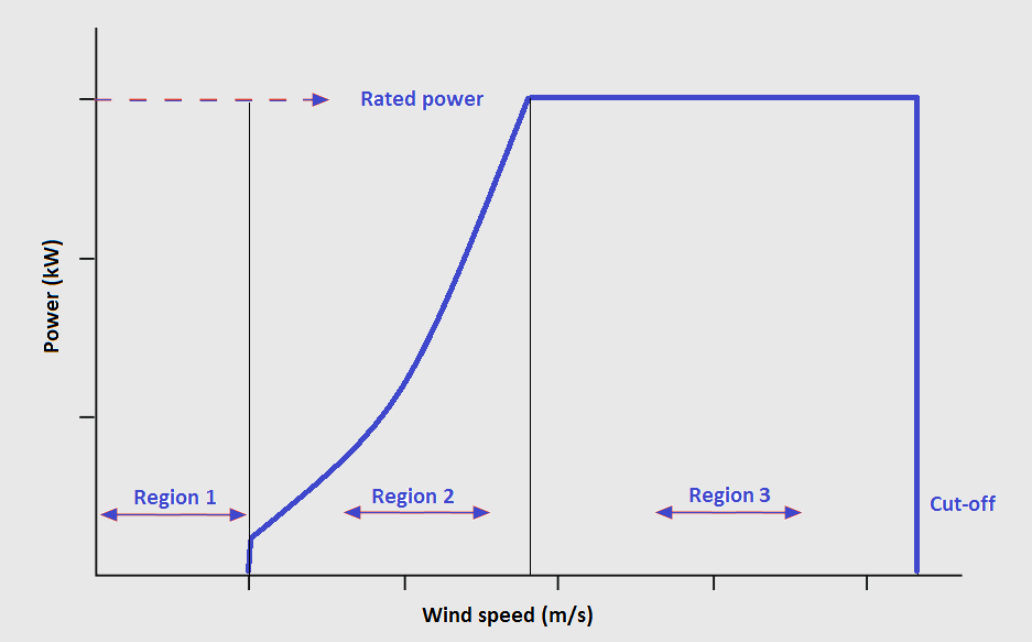

Figure 5: Regions of operation for a wind turbine. In region 2 the objective is to extract as much energy as possible, while in region 3 the objective is to limit power.

2.5 Turbine control mechanisms

There are few to no economic gains by designing the wind turbines to operate in the rare events of unusual high wind speeds. To hinder the overload of turbines in the event of region 3 wind speeds, power output has to be limited. Protection of the structural integrity of the turbines in such scenarios is therefore achieved by different control mechanisms on each wind turbine.

2.5.1 Pitch

The control of pitch is to rotate the blades around its axis such that the wind's angle of attack is changed. This is useful in limiting the peak power, for example, in region 3 operations by slowing down the rotor rotation. If the wind speed reaches a high enough speed, the pitch controller turns (pitches) the blades such that the angle of attack is reduced, this also reduces the lift. In the event of lower wind speeds, the blades are pitched back to optimal angle of attack (wind normal to the largest surface area). This operation is performed while the rotor continues its normal rotation. Previously, the pitch mechanism was hydraulically controlled, this is now being replaced by electrical motors[17]. Pitch control is today usually achieved by using PID pitch control[18]. The pitching of the blades is a relatively slow process, the maximum pitching speed is typically in the range of 5-10 $\frac{deg}{s}$. The pitch speed is dependent of the size of the blades, where larger blades rotate slower than smaller blades. This limit should be taken into account when designing a pitch controller[7].

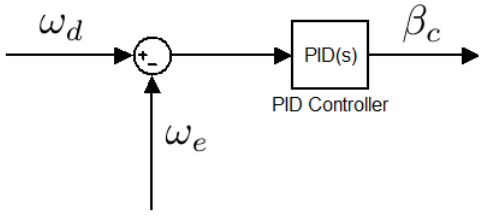

Figure 6: Example of a pitch control scheme

where ω_g is the generator speed, ω_d is the desired generator speed and β_c is the control pitch angle(reference).

2.5.2 Stall

Instead of decreasing the angle of attack one may increase it such that the blade stalls, also called active stall control. By doing this, the blade rotation slows down due to the increase of drag and by the decrease of lift. Stall control is beneficial in gusty wind conditions, see [19] for details. In some types of wind turbines the blades aren't able to pitch, instead the rotor blade angle is fixed. This angle is such that in a given wind region, the stall effect is induced. This is called passive stall control. With passive stall, the power output is reduced

after the wind speed reaches a given threshold; the power output with active stall-control is then flattened out, much like the power curve for active-pitch control.

2.5.3 Yaw

Yaw control is used to rotate the rotor such that it perpendicularly faces the wind stream. The power lost by the turbine yaw error, which is if the rotor is not perpendicular to the wind, is proportional to the cosine of the yaw error angle:

$$P_a = \frac{1}{2}\rho A_d v^3 C_p cos(\theta) \tag{18}$$

where P_a is the total power output from the turbine and θ is the angle between the wind direction and the direction of the rotor. Therefore, when θ is 0, the maximum wind energy is generated.
While yaw control is used to face the rotor perpendicularly towards the wind, it may also be used to decrease power. The main problem of using yaw as a power control method is that the part of the rotor that is closest to the wind is subject to a larger bending torque than the rest of the rotor. Not only does this make the rotor automatically yaw against the wind, it also bends the rotor back and forth cyclically due to the uneven force distribution. Both of these effects induces large fatigue loads and yaw power control is thus only used for smaller wind turbines[17].

3 Wind farms in the electric grid

The demand for electricity will continue to rise and the markets will need to undergo institutional and technical changes. This means that the market must undergo a liberalization process, this opens up for more decentralized and therefore a more flexible power generation from renewable energies. This development has given rise to new opportunities, but also technical challenges for transmission and distribution grid operators.
As a result of the climate and energy crisis, the EU has set a target of 20% of its energy supply to come from wind and other renewable resources by 2020. To meet this target, more than one-third of European electrical demand will need to come from renewable sources, and wind power is expected to deliver 12-14% of the total demand, this equals to approximately to 180 GW. Thus wind energy will play a leading role in providing a steady supply of green power[9].

Traditionally, wind turbines have been treated as a single power generator connected to the power grid where each individual turbine has been controlled to maximize its power output; all of it is delivered to the grid.
The continued research and development efforts in wind energy capture, will lead to challenges in how to integrate wind power on a large scale to the electrical grid. One of the challenges is to maintain system reliability, that is, to secure stable electricity supply and at the same time keep a high penetration levels with low integration cost.

3.1 Uncertainty of wind power generation

Because of the increased fraction of energy produced by wind compared with the total available generation capacity (wind energy penetration), the high variability of electricity generated from wind farms leads to several problems. The instantaneous energy generation must be stable to maintain good grid stability. Traditionally, the individual optimization of each individual turbine, lead to a highly fluctuating output to the grid. Therefore, with the increasing wind power penetration, the wind farms are required to act as a single controllable unit to stabilize the grid output, much like conventional power plants. The total power output is then required to be constant.
In order to be able to track the total wind farm output, the individual wind turbines need to be coordinated, the wind farm controller is in charge of this.

Consequences of this are that wind turbines are often required to operate at a power reference which is lower than the power production limits. This leaves the turbines the option to increase/decrease their power production; these changes in power production can be used to alleviate the wind turbine loads caused by wind turbulence. The power surplus may also be used to improve the wind turbine dynamic operation[7].

3.2 Alternative power system reserves

To prevent loss of electricity in the events of low wind power production, the use of backup energy is needed. Therefore, the determination of alternative reserves in power systems with high wind penetration is given much attention and research. It's not possible to perfectly predict future loads, and generator outputs will vary in different time frames. It is also the possibility that large power system equipment can fail at any time, without any notice. The reserves thus play an important role to assist in generation and load balance, as well as frequency control. Reactive power reserve are also needed to provide voltage support[11]
Hydro power (pumped-storage) has for a long time, been used to level out fluctuations in electricity production and consumption, hence this issue is not completely new and much understood[11]. Hydro power also complements with wind power generation very well, hydroelectricity and also other forms of grid energy storage may store energy generated during high-wind periods, and release this when needed - this help secure a very stable power supply. This is relatively manageable, even though local weather fluctuations vary a lot, the average of the aggregated turbines is quite stable and predictable due to both weather forecasting and the predicted seasonal fluctuations. Different countries may rely on different power system reserves, based on geographical resources and types of power plants available. With the increase of wind penetration, more precise wind forecasting will also add value to wind power and with the increased precision of weather forecasting and modelling, one may lower the requirements for the operational reserves. This is seen in figure 7, which give the contrast between persistence forecasting and perfect forecasting. Persistence forecasting assumes constant output power for one hour ahead. In conclusion, improved weather forecasts and output models are probably one of the key research priority to improve predictability of wind power output.[22]

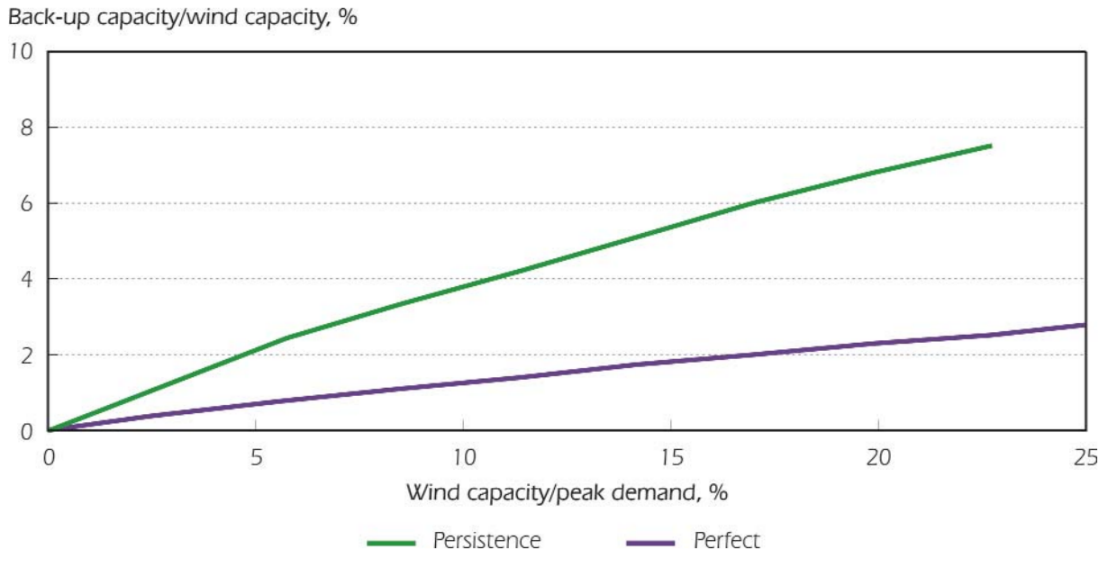

Figure 7: Reduced back-up capacity for improved weather forecasting[22]

3.3 Generators

Because of the varying nature of the wind, the wind turbine generator needs to operate at variable speeds. There are essentially two types of generators commonly used in wind turbines, the synchronous and the asynchronous generator. A synchronous generator use a DC current which is applied to the rotor winding to produce a magnetic field. When the shaft inside the rotor is externally driven, the magnetic field created by the DC current rotates as the same speed as the rotor (n_{rotor}). This creates a changing magnetic flux that passes through the stator windings at the same frequency as the rotor magnetic field rotates. This induces a 3-phase voltage within the stator winding[35]. Wind turbines using synchronous generators use electromagnets in the rotor which are fed by direct current from the electric grid. Since the grid supplies alternating current, it is first converted to DC before it is sent into the coil-winding around the electromagnets. The electromagnets in the rotor are connected to the current by using brushes and slip rings on the shaft of the generator[24]. The frequency of the AC voltages induced across the stator windings of the synchronous generator may be found as:

$$f_{stator} = \frac{n_{rotor} \times N_{poles}}{120} \tag{19}$$

where n_{rotor} is in this case the speed of the synchronous generator rotor, expressed in rotations per minute. N_{Poles} is the number of magnetic poles in the generator per phase.

Asynchronous generator, also known as the induction generator has its name because the rotor has no torque at the precise synchronous rotational speed. The asynchronous generator also consists of two main parts, the stator and the rotor. It is the most used generator type used for wind power. This is because of its robustness and its simple structure. The output frequency of the asynchronous generator is slightly lower than the synchronous speed which may be calculated in the same way as for the synchronous generator, equation 19. This reduction in speed, is usually in around 1% of the synchronous speed[20].
Unless an induction generator is used, it is not possible for it to connect directly onto the electric grid without a frequency transformer. The frequency transformer consists of a rectifier and a inverter. This frequency transformer makes it possible for variable rotational speeds of the turbine when the frequency of the power grid is different[24].

3.4 The doubly-fed induction generator

To ensure frequency control is one of the essential tasks when trying to secure a stable operation of the AC power grid. With the increasing wind penetration, frequency control problems arise and the requirement to perform similar to large synchronous generators are necessary. Technological development regarding control of wind generators allows for a more robust participation in frequency control and therefore enabling a safe increase in wind power penetration.
Doubly fed induction generator (DFIG) wind turbines has become the most widely used

wind turbine for wind farms, since it presents noticeable advantages such as: the variable speed generation, i.e. its ability to produce the required power at varying rotor speeds, the decoupled control of active and reactive powers, the reduction of mechanical stresses and acoustic noise and the improvement of power quality[20]. Figure 8 show a basic diagram of a DFIG with the rotor and grid side converters.

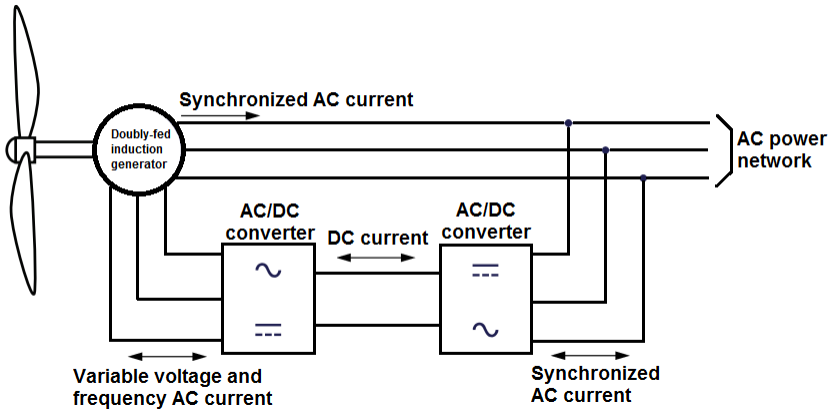

Figure 8: Doubly-fed induction generator.

The basic idea of the induction generator is that the mechanical power at the shaft is converted to electrical power via the stator and rotor windings, it is then supplied to the electrical grid(AC power network). The doubly-fed induction generator, however, operates like a synchronous generator with constant speed that equals the rotation speed which it must rotate to generate power at the AC power network frequency $f_{network}$. This is achieved by feeding AC currents of variable frequency and amplitude to the generator rotor windings. It is thus possible to keep the stator voltage amplitude and frequency constant by adjusting the AC current fed into the rotor windings.

The magnetic field created in the rotor of a DFIG is not static since it is created used three-phase AC current instead of DC current. It does however rotate at a speed $n_{\phi rotor}$ proportional to the frequency given by the AC currents which is fed to the generator rotor windings. The magnetic field that passes through the generator stator windings rotates due to both the rotation of the generator rotor (from external mechanical input) and the rotational effects from the AC current fed from the grid to the generator rotor windings. Therefore both of these determine the frequency f_{stator} of the AC voltage induced across the stator windings.
When the magnetic field at the rotor and the generator rotates in the same direction, the rotor speed n_{rotor} and the speed of the rotor magnetic field $n_{\phi rotor}$ add up. This can be seen from figure 9.

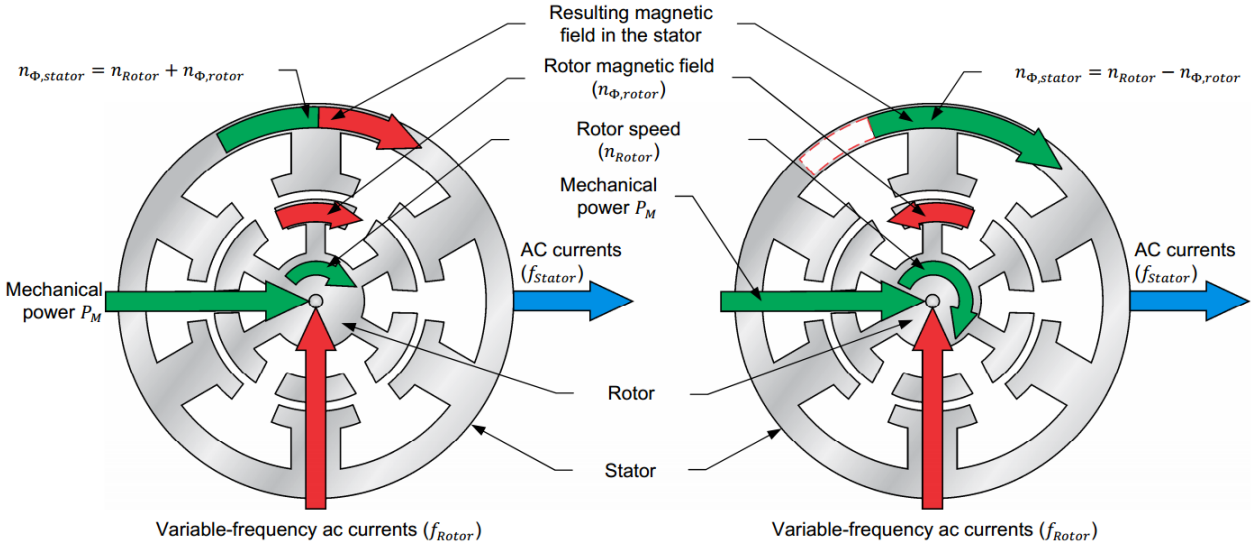

Figure 9: The rotating magnetic field created in both the rotor and stator windings of a doubly-fet induction generator. Source [35].

The frequency of the AC voltages induced across the stator windings is given as:

$$f_{stator} = \frac{n_{Rotor} \times N_{Poles}}{120} + f_{Rotor} \tag{20}$$

where f_{Rotor} is the frequency of the AC current fed in the rotor windings. As seen from figure 9, when the magnetic field at the rotor and the generator rotate in the opposite direction the equation for f_{stator} is:

$$f_{stator} = \frac{n_{Rotor} \times N_{Poles}}{120} - f_{Rotor} \tag{21}$$

3.4.1 Doubly-fed induction generators and wind turbines

The main reason for using doubly-fed induction generators in wind turbines is to produce three-phase AC voltage where the frequency of the voltage across the stator windings f_{Stator} is constant and equals the frequency of the electrical grid $f_{Network}$. This frequency control is as discussed above possible because of the AC currents which are fed into the rotor windings with different frequency and amplitude. By doing this, it is also possible to adjust and control the amount of reactive power and thus to keep the power factor at unity. This also help to counteract or reduce any variations in the amount of electrical power produced due to wind speed bursts. This is what makes it possible to directly connect the generator to the electrical grid. To achieve this frequency control, the AC currents fed into the rotor windings must be continually adjusted to counteract the variation of the rotor speed n_{Rotor}. The frequency of the AC currents f_{Rotor} is dependent on the generator rotation speed n_{Rotor}. We know that

the goal is to keep f_{Stator} equal to $f_{Network}$, thus by using equation 20 and replace f_{Stator} with $f_{Network}$ we may find the desired frequency of the AC current:

$$f_{Rotor} = f_{Network} - \frac{n_{Rotor} \times N_{Poles}}{120} \tag{22}$$

we can see that from 22 that if the generator rotor speed is above the nominal synchronous speed, the frequency of the AC currents must be fed into the magnetic field created in the rotor windings must rotate in the direction opposite to the direction of the rotor. In the case where the generator rotor speed is below the nominal synchronous speed, the polarity of the frequency is positive and the magnetic field must rotate in the same direction as the rotor. When n_{Rotor} rotates at the nominal synchronous speed, the generator operate as a singly-fed three-phase synchronous machine[35].

4 Wind and forecasting

4.1 Characteristics of Wind

Wind is the response to the differential heating of the earth's surface, this creates motion in the air. The wind, which transports both heat and moisture is an important part of the climate since energy is stored in the atmosphere as latent heat.

Wind speed and direction is highly variable, there are several reasons for this, both predictable and unpredictable. The predictable reasons include the diurnal and seasonal heating and cooling. The main diurnal effects consist of the presence of the sun during the day and its absence during night time. The seasonal effect mainly consists of the earth's orbit around the sun. More unpredictable effects consist of the irregular variations in the clouds and mobile weather pressure systems. Local topographic features also influence the air movement. This may be natural or even man-made - any object or surface on the earth modifies the flow of the wind. The different heating characteristics of different surfaces modify the air motion differently. An example is the difference between the temperature of air and water which can cause the breeze often found along the shore-line.
Although the wind is highly unpredictable, there are generally two generalizations regarding the predictability of the wind that should be noted. The first is that wind speed is typically greater in the daytime than at night. As mentioned before, wind is air in motion in response to the differential heating of the earth's surface. Therefore diurnal effects in the wind speed are noticeable close to the earth's surface. As the surface is heated, the wind speed typically increases, and decreases when the surface cools down. Local variations may reduce this diurnal effect, for examples different amount of vegetation may consume different amount of energy due to photosynthesis, among other things. The soil then has less available energy to heat the air. Snow is also a factor that may reduce the diurnal variations, this is because the snow increases the reflection which results in less absorption of solar radiation. Seasonal wind variations are different. During winter, a higher north to south temperature gradient leads to higher wind speeds.
The second generalization is that the wind speed usually increases with the height above the surface. The lower wind speeds near the surface is due to surface friction, the smoothness determine how both the wind speed and direction changes. This is the reason why wind turbines are built high above the surface[37].

Wind speeds may be measured at one anemometer height, this might be lower than the hub height of the wind turbine. It is then necessary to find a way to estimate the wind speed at hub height, typically a power law wind profile is used. The power law is given as:

$$U_2 = U_1 \left(\frac{Z_2}{Z_1} \right)^{\alpha} \tag{23}$$

where:

U_2 = Wind speed at height Z_2

U_1 = Wind speed at height Z_1

Z_2 = computed height

Z_1 = reference height

α = power law exponent

The power law exponent α is a function of surface roughness and stability, empirical studies have found that a value of 0.14 is a value that typically fits most wind farm sites. This method is called the "one-seventh" power law[38].

The importance of large wind turbine towers may be shown by a simple example. If the measurement of the wind speed at a height of 40 meters is 8 m/s. The increase in wind speed at a height of 80 meters would be:

$$U_{80} = 8\left(\frac{80}{40}\right)^{0.14} = 8.815 \text{ m/s} \tag{24}$$

which is an increase of 10.19%. Thus, by doubling the tower height, we may increase the wind speed by around 10% and one may expect the potential power increase by around 34%(this may be calculated using equation 14). This result reinforces the argument of the value of a large wind turbine tower.

4.2 Forecasting

Weather forecasting is the application of science and technology to predict the state of the atmosphere at a given location for a given time in the future. The value of better forecasting is not only limited to a lower requirement for the operational reserves, it also gives a competitive knowledge advantage in the energy market trading, more cost efficient operation, maintenance and planning. The mitigation of the structural impacts of extreme weather is reduced as well as improved worker safety.
When deciding the location of a new wind farm, a number of factors are taken into consideration, but the single most important factor is the meteorological conditions. Because of the massive cost for each wind turbine, once a wind park is built, it is absolutely necessarily with good and stable wind conditions to secure economic viability. While improved forecasting does not eliminate the variability of the wind, it may reduce the uncertainty. Since the wind power output is uncertain in nature and by the increasing wind penetration in the electric grid, it is necessary to schedule the power production, often as far as a day in advance to secure the stability in the power grid by the use of alternative power systems.

Short-term forecasts (1-72h) are useful in power system planning and for trading in the electrical market. Medium-term forecasts and predictions (3-7 days) are needed when planing maintenance of the wind farms and to schedule grid maintenance and energy storage operations[25]. Typically, the forecast errors increase as the time horizon increases.

4.3 Forecasting and prediction methods

Forecasting models for wind power can be divided into two main groups. The first is based on historical time series analysis of the wind, the second group uses forecasted values from a numerical weather prediction (NWP) model as its input. As stated in [25], the wind power forecasting is generally described as physical, traditional statistical or 'black box' methods. More recently the so-called learning approaches, artificial intelligence or 'gray box' methods are being used. The models in the first group forecast power production or mean hourly wind speed by the use of statistical methods. To yield good results, large amount historical time series data is needed.
The second group predicts wind power N-steps ahead mainly by using variables from hourly mean wind speed and its direction which is derived from a meteorological model of the wind dynamics.
The selection of a particular NWP model is an important step in developing the NWP-based wind power prediction. The basis for selecting a certain NWP model includes the geographical area, the forecast horizon, the resolution and the accuracy of the forecast. There are typically three main components of the NWP models: The dynamic center, which represents the adiabatic non-viscous flow, the physical equations which describes the variability of the meteorological processes such as turbulence and radiation, and the information gathering software code. The output of an NWP model is therefore not just the wind, but also a detailed forecast of the atmospheric state at a given time. To further reduce the forecast

error, ensemble forecasting is used, that is to use multiple models to obtain better precision. NWP holds best for time horizons greater than 4 hours. Most models are multi-step and provide look-ahead times for numerous horizons, but the most of these only produce a single expected value for each forecast time scale and are referred to as deterministic(also spot or point) forecasts. Their use for stochastic optimization and risk assessment is therefore limited[25].

4.3.1 Physical methods

The physical models generally use global databases of meteorological measurements or atmospheric mesoscale models. Description of the lower atmosphere is by these methods used to estimate the wind power output. The numerical codes for wind field modelling over rough terrain are generally divided into two types: dynamic and kinematic models. The momentum and energy equations are not solved explicitly, but considered indirectly using parametric relations and/or wind data. To adjust for the local conditions of the terrain, the power law is alternatively adjusted by the use of computational fluid dynamics. Examples of physical approach methods are the Global Forecasting System, MM5, Prediktor and HIRLAM.

4.3.2 Ensemble forecasting

Ensemble forecasting uses multiple models to predict the future prediction outcome. The results are examined and evaluated by its distribution. If the results differ widely, this indicates a large uncertainty. By the use of ensemble forecasting, the reliability and precision of the different methods may also be evaluated. The other way of ensemble forecasting is to use the same model, but to do a number of different model runs to predict several future weather outcomes. As for the multi-model approach, the results are examined by its distribution.

4.3.3 Statistical methods

In the statistical method, the link between historical power production and weather is used to predict and forecast the future power production. The methods used in the statistical methods are described as 'black box'. This is because instead of the approach for physical methods, the statistical approach only involves one-step to go from input to output, and thus the power. There are many different statistical techniques, autoregressive (AR), moving average (MA), autoregressive moving average model (ARMA) and autoregressive integrated moving average models (ARIMA), BOX-Jenkins methodology and the Kalman filter[25].

4.3.4 Learning approach methods

Machine learning methods are also called 'grey box methods' or soft computing approaches. They got their name because they learn without being explicitly programmed. Two examples of machine learning approaches are the Artificial Neural Networks (ANN) and the Support Vector Machines (SVM).

4.4 Steps in choosing a forecast model

1)The first step in forecasting is to define the problem, what do we want to forecast? We need to find out what data we need, in wind power production estimation; wind speed is the most important.
2) The gathering of historical information which is quantified as numerical data.
3) To help in the next step of choosing the model to make the forecast, analysis should be made where correlations and variables should be looked for.
4) Several forecast models are chosen, these models is based on the relevant information from the analysis in the previous step.
5) The results of the models is analysed and the model yielding best results are chosen.

4.5 Models for time series data

4.5.1 The autoregressive(AR) Model

The output variable of the autoregressive model depends linearly on its previous values and is a common model for time series. The model is defined as follows:

We consider the time series $y_1, y_2, ..., y_n$. The order p of an AR model is denoted as $AR(p)$ which states that y_i is a linear function of the previous p values of the series. An error term is also included:

$$y_i = \phi_0 + \phi_1 y_{i-1} + \phi_2 y_{i-2} + ... + \phi_p y_{i-p} + \epsilon_i \quad , for\ i > p \tag{25}$$

where $\phi_1, ..., \phi_p$ are the parameters of the model which we have to determine and ϕ_0 is a constant. ϵ_i white noise, normally distributed with zero mean and variance σ^2.

To fit the AR(1) model:

$$y_i = \phi_0 + \phi_1 y_{i-1} + \epsilon_i \tag{26}$$

we have the observations $y_1, ..., y_n$ which define the linear system of $n-1$ equations:

$$\begin{aligned} y_2 &= \phi_0 + \phi_1 y_1 + \epsilon_2 \\ y_3 &= \phi_0 + \phi_1 y_2 + \epsilon_3 \\ &\vdots \\ y_n &= \phi_0 + \phi_1 y_{n-1} + \epsilon_n \end{aligned} \tag{27}$$

we do a linear regression to find the best values for the parameters $\hat{\sigma}_0$ and $\hat{\sigma}_1$ which then will give us an estimate s^2 for σ^2. Our fitted values for the series are now:

$$\hat{y}_i = \hat{\phi}_0 + \hat{\phi}_1 y_{i-1} \tag{28}$$

we estimate σ^2 by s^2:

$$s^2 = \frac{1}{n-3}\sum_{i=2}^{n}(y_i - \hat{\phi}_0 - \hat{\phi}_1 y_{i-1})^2 \tag{29}$$

The 95% prediction interval for y_i when y_{i-1} is known is:

$$\hat{\phi}_0 + \hat{\phi}_1 y_{i-1} \pm 2s \tag{30}$$

we may forecast n-steps ahead. To find the prediction interval, we have(see [27] for details):

$$y_{n+1} = \hat{\phi}_0 + \hat{\phi}_1 y_{i-1} \quad \pm 2s \tag{31}$$

and

$$y_{n+2} = \hat{\phi}_0 + \hat{\phi}_0 \times \hat{\phi}_1 + \hat{\phi}_1^2 y_n \quad \pm 2s\sqrt{1+\hat{\phi}_0^2} \tag{32}$$

and

$$\begin{aligned} y_{n+3} &= \hat{\phi}_0 + \hat{\phi}_1 y_{n+2} + \epsilon_{n+3} \\ &= \hat{\phi}_0 + \hat{\phi}_1(\hat{\phi}_0 + \hat{\phi}_1 y_{n+1}) + \epsilon_{n+3} \\ &= \hat{\phi}_0 + \hat{\phi}_1(\hat{\phi}_0 + \hat{\phi}_1(\hat{\phi}_0 + \hat{\phi}_1 y_n + \epsilon_{n+1}) + \epsilon_{n+2}) + \epsilon_{n+3} \\ &= \hat{\phi}_0 + \hat{\phi}_0\hat{\phi}_1 + \hat{\phi}_1^2\hat{\phi}_0 + \hat{\phi}_1^3 y_n + \hat{\phi}_1^2\epsilon_{n+1} + \hat{\phi}_1\epsilon_{n+2} + \epsilon_{n+3} \end{aligned} \tag{33}$$

we therefore have:

$$y_{n+3} = \hat{\phi}_0 + \hat{\phi}_1\hat{\phi}_0 + \hat{\phi}_1^2\hat{\phi}_0 + \hat{\phi}_1^3 y_n \pm 2s\sqrt{1+\hat{\phi}_1^2+\hat{\phi}_1^4} \tag{34}$$

the following formula for k-step ahead:

$$y_{n+k} = \hat{\phi}_0\left(\sum_{i=1}^{k}{\phi_1}^{i-1}\right) + {\phi_1}^k y_n + \sum_{i=1}^{k}{\phi_1}^{i-1}\epsilon_{n+k-i-1} \tag{35}$$

the last summation is the error term where the rest is the forecast.

4.5.2 The Moving Average(MA) model

A moving average model of order q, MA(q), is a time series model defined as:

$$y_t = \psi_0 - \psi_1\epsilon_{t-1} - \psi_2\epsilon_{t-2}, ..., \psi_q\epsilon_{t-q} + \epsilon_t \tag{36}$$

where $\psi_0, \psi_1, ..., \psi_q$ are constants and ϵ_t is Gaussian white noise, normally distributed with mean 0 and variance σ^2: $\mathcal{N}(0, \sigma^2)$. Thus the moving average model use past forecast errors instead of the past values. ϵ_0 is by convention set to 0.

To estimate the constants, we can write up a set with n equations, we assume we have n values of a time series $y_1, ..., y_n$. This example is for the simple MA(1) model.

$$\begin{aligned} y_1 &= \psi_1\epsilon_0 + \epsilon_1 = \epsilon_1 \\ y_2 &= \psi_1\epsilon_1 + \epsilon_2 = \psi_1 y_1 + \epsilon_2 \\ y_3 &= \psi_1\epsilon_2 + \epsilon_3 = \psi_1(y_2 - \psi_1 y_1) + \epsilon_3 \\ &\vdots \\ y_n &= \psi_1\epsilon_{n-1} + \epsilon_n = \psi_1 y_{n-1} - {\psi_1}^2 y_{n-2} + ... + (-\epsilon_1)^{n-1} y_1 + \epsilon_n \end{aligned} \tag{37}$$

the systems of equations is non-linear.

4.5.3 ARMA

In the ARMA model we combine the AR and MA models. We define the ARMA(p,q) model, where p and q is the order of the AR and MA models, respectively:

$$y_t = \phi_0 + \phi_1 y_{t-1} + ... + \phi_p y_{t-p} + \psi_0 - \psi_1\epsilon_{t-1} - ... - -\psi_q\epsilon_{t-q} + \epsilon_t \tag{38}$$

ϕ_0 and ψ_0 can be summed and this product may be defined as the constant c:

$$y_t = c + \phi_1 y_{t-1} + ... + \phi_p y_{t-p} - \psi_1\epsilon_{t-1} - ... - -\psi_q\epsilon_{t-q} + \epsilon_t \tag{39}$$

The problem with ARMA models is that they doesn't handle time series that are not stationary in mean and variance, that is, one should not use ARMA models with time series that have trends or seasonal patterns.

4.5.4 ARIMA

A time series which is stationary in mean does not include a trend, and is good for the ARMA model. However, if a trend or seasonal patterns is present, we need to include differencing

to remove this.
If we consider a time series y_t, first order differencing is:

$$\frac{dy_t}{dt} = y_t - y_{t-1} \tag{40}$$

for a compact notation, we can introduce the back-shift operator B, defined as:

$$\frac{dy_t}{dt} = y_t - y_{t-1} = y_t - By_t = (1 - B)y_t \tag{41}$$

This differencing is then integrated into the ARMA models. ARIMA(p,d,q) defines the model where p,q is the order of the AR, MA model, respectively and d is the order of the differencing applied[27].

$$(1 - \phi_1 B - \phi_2 B^2 - ... - \phi_p B^p)(1 - B)^d y_t = c + (1 - \psi_1 B - \psi_2 B^2 - ... - \psi_q B^q)\epsilon_t \tag{42}$$

4.6 The Kalman filter

This statistical method establishes a state-space model where the wind speed is set as the state variable, the filter then may predict the future value of the wind speed. The discrete Kalman filter procedure is briefly described with the extension to its use as a forecasting method[29].

The unknown process to be estimated is given as the system equations form:

$$\mathbf{x_{k+1}} = \mathbf{\Phi_k x_k} + \mathbf{w_k} \tag{43}$$

where $\mathbf{x_k}$ is the process state vector at time k and $\mathbf{\Phi_k}$ is a transition matrix which relates $\mathbf{x_k}$ to $\mathbf{x_{k+1}}$. $\mathbf{w_k}$ is a vector given as white noise with known covariance structure.
The measurement $\mathbf{z_k}$ at time k of the process is given as:

$$\mathbf{z_k} = \mathbf{H_k x_k} + \mathbf{v_k} \tag{44}$$

where $\mathbf{H_k}$ give the relation between the state and the measurement at time k. $\mathbf{v_k}$ is the measurement error, it is assumed to be white noise with known covariance and zero cross-correlation with $\mathbf{w_k}$.

The covariance matrices for $\mathbf{w_k}$ and $\mathbf{v_k}$ are:

$$\mathbf{E}[\mathbf{w_k}\mathbf{w_i}^\mathbf{T}] = \begin{cases} Q_k, & \text{i } = \text{k} \\ 0 & \text{i } \neq \text{k} \end{cases} \tag{45}$$

$$\mathbf{E}[\mathbf{v_k}\mathbf{v_i}^{\mathbf{T}}] = \begin{cases} R_k, & \text{i } = \text{k} \\ 0 & \text{i } \neq \text{k} \end{cases} \tag{46}$$

$$\mathbf{E}[\mathbf{w_k}\mathbf{v_i}^{\mathbf{T}}] = \mathbf{0}, \quad \text{for all k and i} \tag{47}$$

We have an estimation error at t_k:

$$\mathbf{e_k^-} = \mathbf{x_k} - \hat{\mathbf{x}}_\mathbf{k}^- \tag{48}$$

where $\hat{\mathbf{x}}_\mathbf{k}^-$ is the a priori estimate. The "hat" denotes estimate, and the "super minus" is a reminder that this is the best estimate prior to assimilating the measurement at t_k.
We also assume that we know the error covariance matrix associated with $\hat{\mathbf{x}}_\mathbf{k}^-$, given as:

$$\mathbf{P_k^-} = \mathbf{E}[\mathbf{e_k^-}\mathbf{e_k^-}^{\mathbf{T}}] = \mathbf{E}[(\mathbf{x_k} - \hat{\mathbf{x}}_\mathbf{k}^-)(\mathbf{x_k} - \hat{\mathbf{x}}_\mathbf{k}^-)^{\mathbf{T}}] \tag{49}$$

With the assumption of a prior estimate $\hat{\mathbf{x}_\mathbf{k}^-}$, we use the measurement $\mathbf{z_k}$ to improve the estimate:

$$\hat{\mathbf{x}}_\mathbf{k} = \hat{\mathbf{x}}_\mathbf{k}^- + \mathbf{K_k}(\mathbf{z_k} - \mathbf{H_k}\hat{\mathbf{x}}_\mathbf{k}^-) \tag{50}$$

where $\hat{\mathbf{x}_\mathbf{k}}$ is the updated estimate and $\mathbf{K_k}$ is the Kalman gain. The problem is to find the Kalman gain that yields an updated estimate that is optimal. The minimum mean-square error is used as the performance criterion.
First, we form the expression for the error covariance matrix:

$$\mathbf{P_k} = \mathbf{E}[\mathbf{e_k}\mathbf{e_k^T}] = \mathbf{E}[(\mathbf{x_k} - \hat{\mathbf{x}}_\mathbf{k})(\mathbf{x_k} - \hat{\mathbf{x}}_\mathbf{k})^{\mathbf{T}} \tag{51}$$

Next, the equation EQ is substituted into equation EQ, we then substitute the resulting expression for $\hat{\mathbf{x}}_\mathbf{k}$ into equation EQ. We then get:

$$\mathbf{P_k} = \mathbf{E}\{[(\mathbf{x_k} - \hat{\mathbf{x}}_\mathbf{k}^-) - \mathbf{K_k}(\mathbf{H_k}\mathbf{x_k} + \mathbf{v_k} - \mathbf{H_k}\hat{\mathbf{x}}_\mathbf{k}^-)][(\mathbf{x_k} - \hat{\mathbf{x}}_\mathbf{k}^-) - \mathbf{K_k}(\mathbf{H_k}\mathbf{x_k} + \mathbf{v_k} - \mathbf{H_k}\hat{\mathbf{x}}_\mathbf{k}^-)]^{\mathbf{T}}\} \tag{52}$$

By performing the expectation and by noting that the $(\mathbf{x_k} - \hat{\mathbf{x}}_\mathbf{k}^-)$ is the a priori estimation error which is uncorrelated with the measurement error $\mathbf{v_k}$, we have:

$$\mathbf{P_k} = (\mathbf{I} - \mathbf{K_k}\mathbf{H_k})\mathbf{P_k^-}(\mathbf{I} - \mathbf{K_k}\mathbf{H_k})^{\mathbf{T}} + \mathbf{K_k}\mathbf{R_k}\mathbf{K_k^T} \tag{53}$$

We wish to find the particular Kalman gain $\mathbf{K_k}$ that minimizes the individual terms along

the diagonal of $\mathbf{P_k}$, this is because these terms represent the estimation error variances for the elements of the state vector that is estimated. In [29], the optimization is done by a straightforward differential calculus approach, which is omitted here. By setting the derivative equation to zero and solve for the optimal gain, the result is given as:

$$\mathbf{K_k} = \mathbf{P_k^-}\mathbf{H_k^T}(\mathbf{H_k}\mathbf{P_k^-}\mathbf{H_k^T} + \mathbf{R_k})^{-1} \tag{54}$$

this is the Kalman gain, which minimizes the man-square estimation error.

We can now derive the error covariance matrix for the updated estimate. By re-arranging equation 53 we have:

$$\mathbf{P_k} = \mathbf{P_k^-} - \mathbf{K_k}\mathbf{H_k}\mathbf{P_k^-} - \mathbf{P_k^-}\mathbf{H_k^T}\mathbf{K_k^T} + \mathbf{K_k}(\mathbf{H_k}\mathbf{P_k^-}\mathbf{H_k^T} + \mathbf{R_k})\mathbf{K_k^T} \tag{55}$$

by substituting the expression for the Kalman gain into equation 55 we may, as described in [29] arrive at three different equation with different numerical performance(including equation 53), we state the most common one here, which is:

$$\mathbf{P_k} = (\mathbf{I} - \mathbf{K_k}\mathbf{H_k})\mathbf{P_k^-} \tag{56}$$

By ignoring the contribution of $\mathbf{w_k}$ in equation 43 because it has zero mean and not correlated with its previous values, we have:

$$\hat{\mathbf{x}}_{\mathbf{k+1}}^- = \phi_\mathbf{k}\hat{\mathbf{x}}_\mathbf{k} \tag{57}$$

We obtain the error covariance matrix associated with $\hat{\mathbf{x}}_{\mathbf{k+1}}^-$ by the expression for the a priori error $\mathbf{e}_{\mathbf{k+1}}^-$, which is:

$$\begin{aligned} \mathbf{e}_{\mathbf{k+1}}^- &= \mathbf{x_{k+1}} - \hat{\mathbf{x}}_{\mathbf{k+1}}^- \\ &= \phi_\mathbf{k}\mathbf{x_k} + \mathbf{w_k}) - \phi_\mathbf{k}\hat{\mathbf{x}}_\mathbf{k} \\ &\quad \phi_\mathbf{k}\mathbf{e_k} + \mathbf{w_k} \end{aligned} \tag{58}$$

Because $\mathbf{w_k}$ is the process noise for the step ahead of $\mathbf{t_k}$ and $\mathbf{w_k}$ and $\mathbf{e_k}$ have zero cross correlation, we can write the expression for $\mathbf{P}_{\mathbf{k+1}}^-$ as:

$$\mathbf{P}_{\mathbf{k+1}}^- = \mathbf{E}[\mathbf{e}_{\mathbf{k+1}}^-\mathbf{e}_{\mathbf{k+1}}^{-\mathbf{T}}] = \mathbf{E}[\phi_\mathbf{k}\mathbf{e_k} + \mathbf{w_k})(\phi_\mathbf{k}\mathbf{e_k} + \mathbf{w_k})^\mathbf{T}] = \phi_\mathbf{k}\mathbf{P_k}\phi_\mathbf{k}^\mathbf{T} + \mathbf{Q_k} \tag{59}$$

We now summarize the equations that comprise the Kalman filter recursive equations:

$$\hat{\mathbf{x}}_\mathbf{k} = \hat{\mathbf{x}}_\mathbf{k}^- + \mathbf{K_k}(\mathbf{z_k} - \mathbf{H_k}\hat{\mathbf{x}}_\mathbf{k}^-) \tag{60a}$$
$$\mathbf{P_k} = (\mathbf{I} - \mathbf{K_k}\mathbf{H_k})\mathbf{P}_\mathbf{k}^- \tag{60b}$$
$$\mathbf{P}_{\mathbf{k+1}}^- = \phi_\mathbf{k}\mathbf{P_k}\phi_\mathbf{k}^\mathbf{T} + \mathbf{Q_k} \tag{60c}$$
$$\hat{\mathbf{x}}_{\mathbf{k+1}}^- = \phi_\mathbf{k}\hat{\mathbf{x}}_\mathbf{k} \tag{60d}$$
$$\mathbf{K_k} = \mathbf{P}_\mathbf{k}^-\mathbf{H}_\mathbf{k}^\mathbf{T}(\mathbf{H_k}\mathbf{P}_\mathbf{k}^-\mathbf{H}_\mathbf{k}^\mathbf{T} + \mathbf{R_k})^{-\mathbf{1}} \tag{60e}$$

Figure 10 shows the equations and the sequence of computational steps.

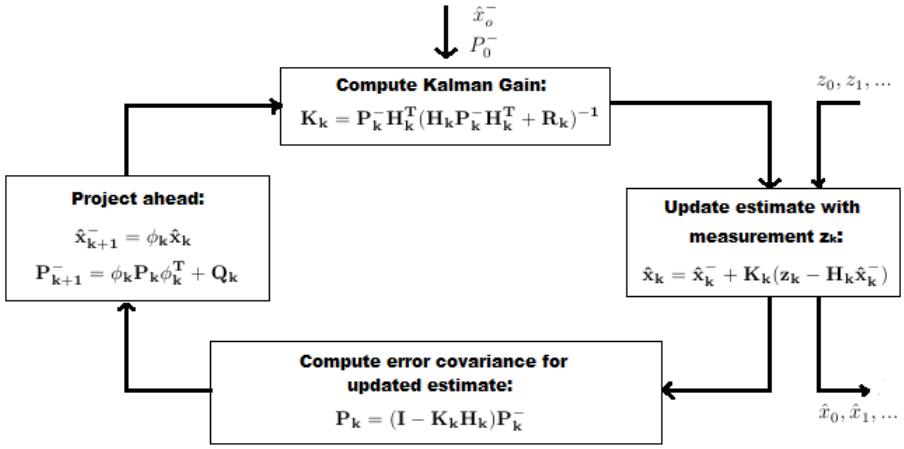

Figure 10: Kalman filter loop

Kalman Filter and Prediction

We may note that the projection operation in figure 10 is a one step prediction. This was based on the assumption of white noise $\mathbf{w_k}$ sequence given in the process model. Instead of just one step, the same argument may be used for projecting N steps ahead of the measurement. The N-step prediction is given as:

$$\hat{\mathbf{x}}(\mathbf{k+N}|\mathbf{k}) = \phi(\mathbf{k+N}, \mathbf{k})\hat{\mathbf{x}}(\mathbf{k}|\mathbf{k}) \tag{61a}$$
$$\mathbf{P}(\mathbf{k+N}|\mathbf{k}) = \phi(\mathbf{k+N}, \mathbf{k})\mathbf{P}(\mathbf{k}|\mathbf{k})\phi^\mathbf{T}(\mathbf{k+N}, \mathbf{k}) + \mathbf{Q}(\mathbf{k+N}, \mathbf{k}) \tag{61b}$$

where:

$\hat{\mathbf{x}}(k|k)$ = updated filter estimate at time t_k.

$\hat{\mathbf{x}}(k+N|k)$ = predictive estimate of $\mathbf{x}$ at time t_{k+N} given all the measurements through t_k.
$\mathbf{P}(k|k)$ = error covariance associated with the filter estimate $\mathbf{x}(k|k)$.
$\mathbf{P}(k+N|k)$ = error covariance associated with the predictive estimate $\mathbf{x}(k+N|k)$.
$\phi(k+N,k)$ = transition matrix from step k to k + N.
$\mathbf{Q}(k+N,k)$ = covariance of the cumulative effect of white-noise inputs from step k to step k + N.

In off-line analysis work, the $\mathbf{P}(k+N|k)$ is the matrix of the most interest as the terms along the major diagonal give a measure of the quality of the predictive state. In on-line prediction it is $\mathbf{x}(k+N|k)$ that is of the most interest. More details and examples may be found in [29].

4.7 Artificial Neuron Network weather prediction

A neural network is a mathematical model inspired by biological neural networks, much like the ones that exist in the human brain. A neural network is a powerful data modelling tool that is able to perform intelligent tasks, it works like an adaptive system which changes its structure during a learning phase. Neural networks are used for modelling complex relationships between input and output or to find patterns. The artificial neuron is quite simple, signals may be 1 or -1, the neuron calculates a weighted sum of inputs which it compares to some threshold value. The output is either set to 1 or -1 depending if the weighted sum is more or less than the threshold value. The structure of a simple neuron can be seen in figure 11.

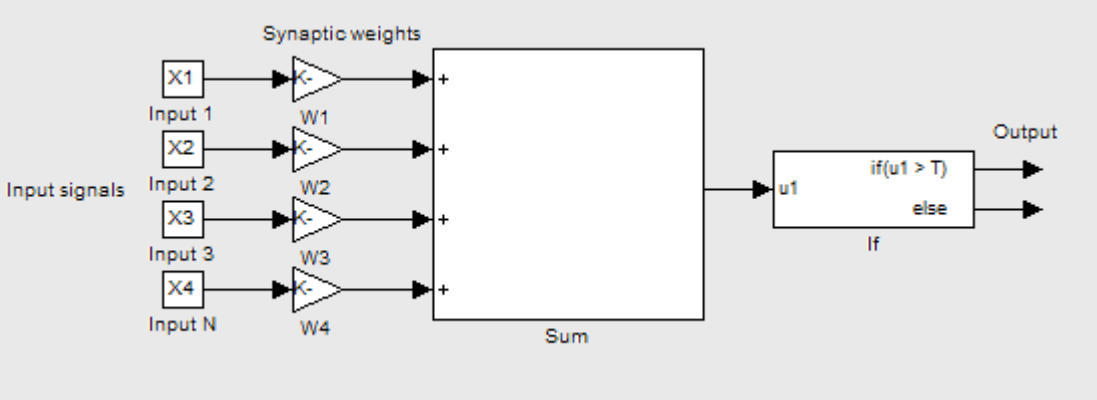

Figure 11: Artificial neuron

The weights in the artificial neuron are called synaptic weights - the knowledge of the neural network is stored in these weights. It is after the neural network has gone through a successful training it is capable to perform prediction, estimation or simulation of data (from data similar to which it was trained with). Artificial neuron networks works much like people in that it learns by example. Also learning in biological systems adds adjustments to synaptic connections between neurons, in the same manner the ANN's knowledge is stored in the synaptic weights.

In [26], a method is suggested where an artificial neural network is used in combination with a so called rule extraction, where a decision algorithm named ID3 is used for this. The ID3 use the output from the neural network and generate rules for prediction. The weather prediction system is given as two phases:

Phase 1: ANN Approach

1. Weight initialization in first step.
2. Input supply.
3. Get output.

4. Get error.
5. Adjust weights of input and hidden layer.
6. Repeat step 4,5 until desired goal not found.
7. Store the output.

Phase 2: Decision Tree

The output from the neural network is supplied to ID3 (Make tree function building).

1. Calculate entropy.
2. Calculate info gain.
3. Choose best attribute.
4. Mount as root.
5. Select next best attribute and so on.

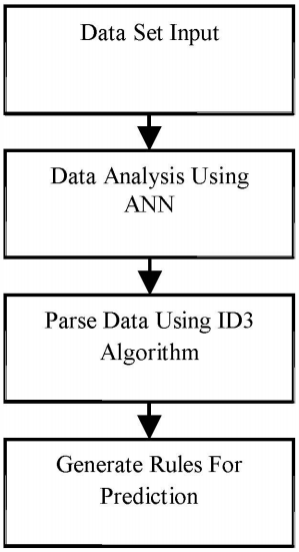

Figure 12: System structure[26]

The input information for a artificial neural network for weather forecasting could typically be: the wind velocity, wind direction, relative humidity, atmospheric pressure and temperature.

5 Wake effects and interactions

There are plans of annual installations of 16.8GW of wind power to satisfy the EU's 2020 targets[8]. This annual increase in wind turbine density and thus larger wind farms leads to smaller spacing between them.

These farms will obviously help reduce the average wind cost of energy (COE). Good wind farm planning is then important, an optimal wind farm layout will help maximize the energy yield and at the same time minimize the number of wind turbines used at the constrained area. They will also introduce the problem of aerodynamic interaction among the turbines, this can decrease the total energy converted to electricity, compared to the same number of isolated turbines under the same wind flow conditions[1].

Because of the reduced spacing between the wind turbines, operating conditions in such wind farms are highly coupled due to the wake interactions from upstream turbines.
A downstream turbine which is affected by the wake will produce reduced amount of power. This interference by the wakes obviously creates a big challenge for the wind farm planners, the wind behind a turbine has lower speed due to the absorbed kinetic energy, other wake effects are strong wind shear and turbulence. Because of these effects, detailed knowledge of the wind flow behind wind turbines is needed for planning and control of large wind farms. Apart from the loss in energy production, an additional negative effect is formed by the increase in turbulence intensity, which is higher fatigue loads on the materials. With regard to the minimisation of wake effects, two approaches can be distinguished[3]:

- Accept the wake effects as they are and try to optimize the wind farm layout in order to suffer as little as possible from these wake effects.

- Reduce the wake effects using dedicated control concepts.

By using an accurate wake model, both of these strategies can be applied simultaneously.
The aerodynamic interaction among the turbine in an array decreases as their spacing increases. When the downwind spacing is 8-10 or more rotor diameters, and the crosswind spacing is around 5 rotor diameters, the array losses may be 10% or less under typical inflow conditions. However, such spacing conditions are not always possible due to various geographical and weather conditions. Hence, there is substantial benefits to be gained from accurate modelling of the wakes behind the wind turbines in a wind farm. This will lead to the minimization of both power losses, turbine spacing and also turbine fatigue loading. Crosswind spacing is usually not as large as the downwind spacing, which means that in locations where the wind direction is from other angles than the prevailing wind direction, array losses are greater[1], see figure 13.

There are obvious economical reasons to place the turbines as close as possible, and the usual methodology used is to select the downwind and crosswind spacing based on the prevailing wind direction and the local topography. In populated areas, the placement is also constrained by noise pollution and aesthetics. Seasonal changes often change the direction of the prevailing wind direction, coordinated control is then absolutely necessary to keep a stable power production.
The wind farm array efficiency is defined as:

$$\eta_A = \frac{E_a}{E_T N} \tag{62}$$

Where the annual energy from the wind farm is E_A, the annual energy captured from one turbine is E_T, and N is the total number of wind turbines.

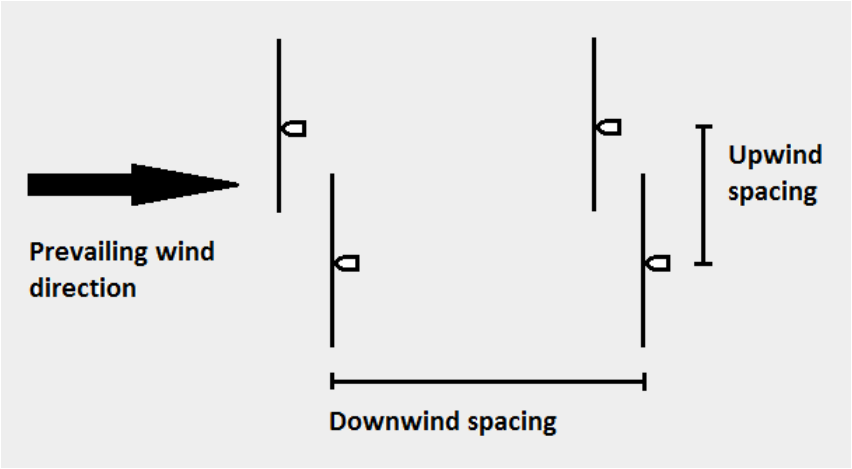

Figure 13: Arrangement of a typical wind farm where the downwind spacing is larger than the crosswind spacing.

5.1 Reduction of individual turbine power

By adapting the level of power production of the wind turbine, the intensity of the wakes may be influenced. This reduction of power reference of an upwind turbine will decrease the above mentioned effects from the wake, and thus the downwind turbine may increase its power production. The wake effects from one upwind turbine may also affect several downwind turbines. As is mentioned in [8], a reduction in the mean power production of the front row of turbines, which are first reached by the wind, one can obtain an increase in the overall wind farm power production. This may reduce the maintenance costs and also extend the service life of the front row turbine. This will also lower the total price of the produced power from the wind farm.

5.2 Wake models and simulation

The first step in simulating new control strategies for the wind farm, is to obtain models which is suitable to on-line optimization. The literature implies that the result from even the most sophisticated, computationally-expensive models varies from the actual interaction among the turbines[1], it is therefore probably acceptable to use more basic models for on-line-optimization via simulation. Wake models are used to predict the wind profile downwind of the turbine.

Wind wakes are typically divided in a near wake and a far wake. The near wake is where the influence of each rotor blade may be distinguished, the swirling vortices will thus make a special contribution. The near wake model calculations are typically too intensive to use in wind farm simulation and calculation. For our purpose where we are interested in the interaction between the wind turbines in the grid, the far wake is the most interesting

There are three different kinds of wake models; numerical, kinematic and field models. In the numerical wake models, wind turbines are described as distributed roughness elements. Field models is based on solving a simplified version of the Reynolds averaged Navier-Stokes flow equations, where it calculates the flow everywhere in the wake.[4]
The aerodynamic interaction among turbines are dependent on the wind direction, this is due to the spatial arrangement of turbines in the wind farm.

5.3 Kinematic models

Kinematic wake models are based on self-similar velocity deficit profiles obtained from experimental and theoretical work on co-flowing jets. The wake description starts after the expansion of the wake and is assigned to two types of velocity profiles: the near, and the far wake with a transition phase in between. The conservation of momentum is often used to model the velocity deficit of the wake where the thrust coefficient is used as input[4]. The wake expansion is due to the ambient turbulence and the turbulence from the shear in the wake. Not all kinematic models use the turbulence as input, such as the Jensen wake model(also called Park model), it assumes a linear wake expansion. Park wake model is based on classical wake theory. An other kinematic wake model, which is described below is not expanding linearly, and thus use the turbulence as input, it is more precise, but not as easy to implement as the Park model.

5.4 Field models

Field models calculate the complete flow magnitude at every point of the flow field by solving the Reynolds-averaged Navier-Stokes equations. Two field models will be described, first the two-dimensional field model of J.F.Ainlie, then the three-dimensional WAKEFARM model. Field models also use a turbulence model.

5.5 The Park Wake Model

This model was developed by N.O.Jensen and Katic et al[1]. The Park wake model is quite simple and effective for simulation, the diameter of the wake is expanding in a linear manner. The model assumes an initial velocity deficit immediately behind the turbine rotor, this is calculated from the turbine's thrust coefficient $C_T = 4a(1-a)$ and the wake-decay constant k. The wake velocity deficit is dependent only on the distance behind the rotor. The effects of multiple wakes are handled by overlapping or superimposing the cross sections of the upstream turbines. See figure 14.

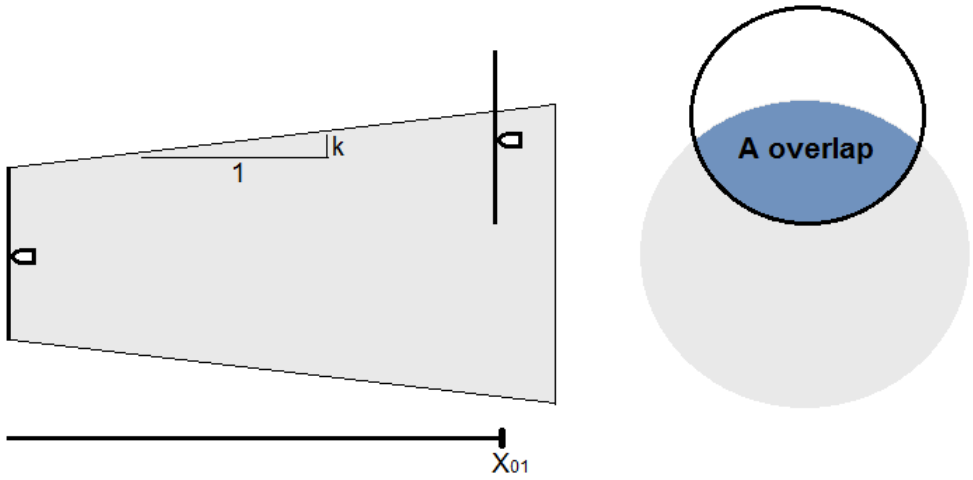

Figure 14: The figure shows the wake expansion and the area of overlap which is used in the calculation of the wake velocity deficit.

The wind speed deficit at the downwind turbine is calculated as follows:

$$\delta V_{01} = V_\infty(1 - \sqrt{1 - C_T}) \left(\frac{D_0}{D_0 + 2kX_{01}}\right)^2 \frac{A_{overlap}}{A_1} \tag{63}$$

where $\frac{A_{overlap}}{A1}$ is the overlap factor, where A_1 is the area of the wind turbine and $A_{overlap}$ is the area where the wake and the incident rotor disc intersects. D_0 is the rotor diameter, k is the wake decay constant and X_{01} is the downstream horizontal distance between the wind turbines[1], see figure 14. The incident wind speed V_i for each turbine is the free-stream wind speed V_∞ minus the wake deficit calculated as $V_i = V_\infty - \delta V_{01}$. As we can see from figure 14, the rate of the wake expansion is k. The wake decay constant k is both determining the rate at which the speed deficit in the wake changes and also the rate of the wake expansion.

Since the Park wake model doesn't include a turbulence model, it is easy to understand that it is important to choose the correct value of the wake decay constant before attempting any simulation. The value k must thus take the roughness of the terrain and other variable factors into consideration to give accurate results. This will be discussed in the last chapter.

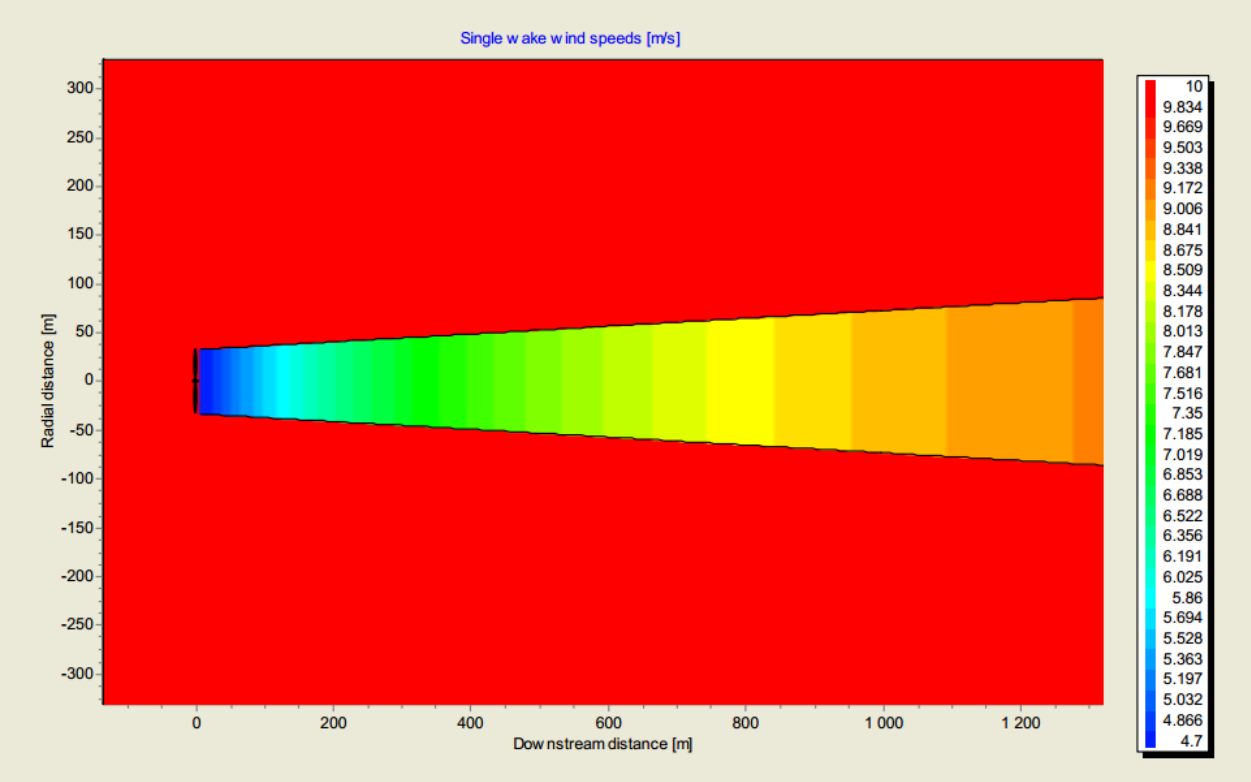

Figure 15: Wake development from the Park wake model, source: [16]

5.5.1 Modified Park Model

This modification to the Park model was developed by Garrad Hassan and Partners, Ltd[23]. It is a simple modification to how to calculate the area of overlap. Instead of calculating the area of overlap as the area of intersection of the wake and the incident rotor disk, the fraction of horizontal overlap is calculated. This fraction is then multiplied by the velocity deficit in the same way as the original method.

5.5.2 Multiple Wake Calculations

Katic et al. suggests that multiple wakes are calculated through the 'sum of squares of velocity deficits' wake combination model[16]. The effects from multiple wakes is found as:

$$\delta V_n = \sqrt{\sum_{k=1}^{n-1} (\delta V_{kn})} \tag{64}$$

The calculation procedure is given as:

1. Start the calculation with the turbine at the most upstream position.
2. Find the wind speed at this turbine.
3. Calculate wind speeds for all downstream turbines.
4. If the downstream turbine is partially in a wake, then reduce the velocity deficit the same way as described in The Park/Modified Park model.
6. Go to the next turbine, and do the same procedure from step 1.

5.6 The Larsen Wake Model

The model is a semi analytical model and derived from asymptotic expressions from Prandtl's rotational symmetric turbulent boundary layer equations. Because of this, the model might be somewhat conservative for close spacings[16].

The wake radius is given as:

$$R_w(x_{01}) = \left[\frac{35}{2\pi}\right]^{\frac{1}{5}} \left[3c_1^2\right]^{\frac{1}{5}} \left[C_T A(x_{01}+x_0)\right]^{\frac{1}{3}} \tag{65}$$

where c_1 is a non-dimensional mixing length given as:

$$c_1 = l(C_T A x)^{\frac{-1}{3}} \tag{66}$$

l is Prandtl's mixing length.
According to [16], the parameter c_1 does to some degree seperate the rotor drag dependence and is therefore expected to be relatively insensitive to the size and design of the rotor.

The position of the rotor with respect to the coordinate system x_0, is given as:

$$x_0 = 9.5D \Big/ \left(\left(\frac{2R_{9.5}}{D}\right)^3 - 1\right) \tag{67}$$

The parameter $R_{9.5}$ is the wake radius at a distance 9.5 rotor diameter downstream and is determined as:

$$R_{9.5} = 0.5\left[R_{nb} + min(h, R_{nb})\right] \tag{68a}$$
$$R_{nb} = max(1.08D, 1.08D + 21.7D(I_a - 0.05) \tag{68b}$$

where I_a is the ambient turbulence intensity at hub height. Equation 68a accounts for the ground blockage effects if the wake radius is larger than the hub height. The Larsen wake model is in contrast to the Park wake model dependent on the ambient turbulence intensity I_a and the hub height H. The mean wind velocity deficit is determined from the expression:

$$\delta V = -\frac{V_\infty}{9}\left(C_T A(x+x_0)^{-2}\right)^{\frac{1}{3}} \left[r^{\frac{3}{2}}\left(3c_1^2 C_T A(x+x_0)\right)^{-\frac{1}{2}} - \left(\frac{35}{2\pi}\right)^{\frac{3}{10}} (3c_1^2)^{-\frac{1}{5}}\right]^2 \tag{69}$$

where r is the radial distance from the wake centerline SE FIGUR(REFERER(bruke [4] som inspirasjon).

The Larsen wake model also includes the option of a first-order and a second-order approximate solution to the boundary layer equations. The second-order description is a semi-empirical near wake description which enables us to model the wake with a "double peak" velocity profile. Only the near wake is modified at the cost of a more computationally intensive expression, thus for many applications, only the first order wake model is needed. See figure 16 for a plot of the wake development of the first-order case.

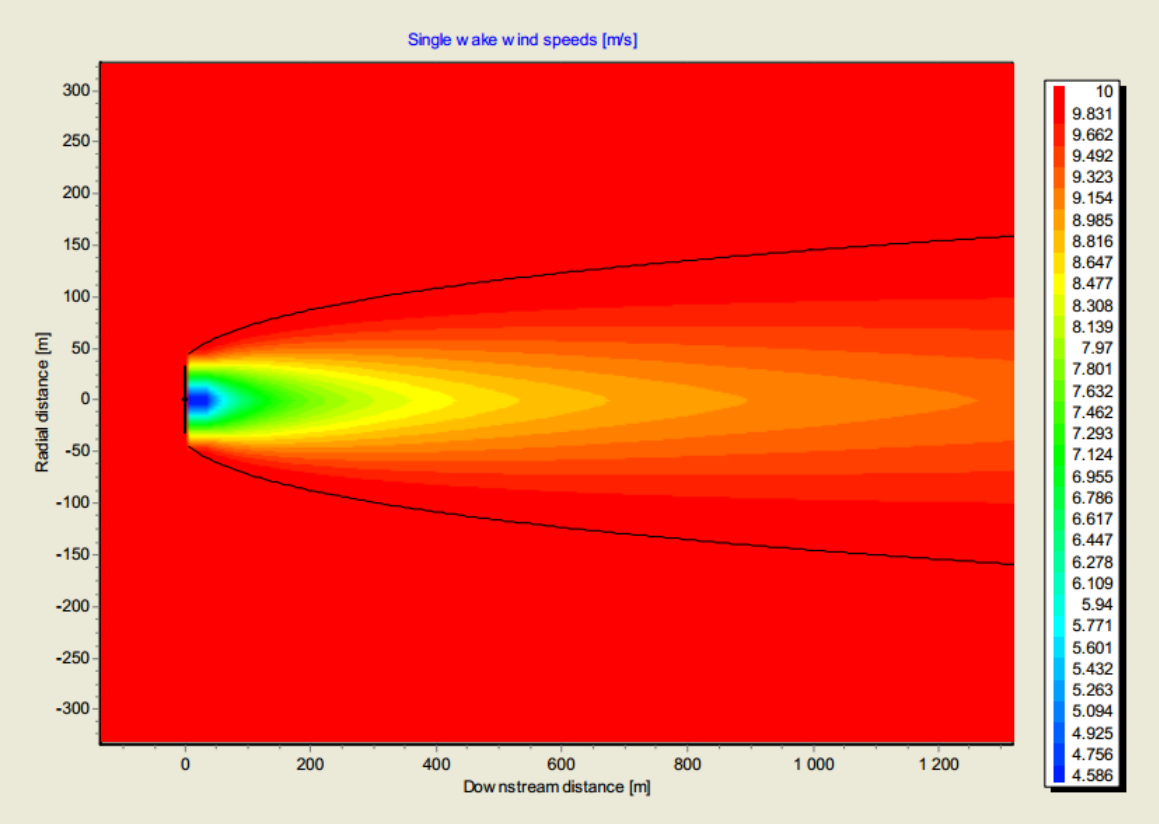

Figure 16: Wake development from the Larsen wake model, source: [16]

5.7 Ainslie model

This is a two-dimensional field model, it assume axial symmetry in the wakes and therefore only calculates the flow through half of the rotor as seen from figure FIG! This simplifies the problem compared to three-dimensional field models, thus less computation time is needed due to the fewer equations to be solved simultaneously. Cylindrical coordinates are used and incompressible fluid flow is assumed.
The continuity equation in cylindrical coordinates is[16]:

$$\frac{1}{r}\frac{\partial rv}{\partial r} + \frac{\partial u}{\partial x} = 0 \tag{70}$$

Using cylindrical coordinates in the thin layer approximation, the Navier Stokes equation are:

$$u\frac{\partial}{\partial x} + v\frac{\partial u}{\partial r} = -\frac{1}{r}\frac{\partial(r\bar{u}\bar{v})}{\partial r} \tag{71}$$

The right side of the equation describes the change in acceleration and thus the momentum. The part is due to the change in momentum caused by the turbulent fluctuations, it's not possible to describe this contribution by using velocities in the averaged flow.
The interactions between mean flow and turbulent eddies is described by the eddy viscosity, also called the turbulent exchange coefficient for momentum[16], and is given as:

$$-\bar{u}\bar{v} = \epsilon(x)\frac{\partial u}{\partial r} \tag{72}$$

Ainslie described the eddy viscosity $\epsilon(x)$ by a length scale $L(x)$, a velocity scale $U(x)$ and the contribution from ambient turbulence to the eddy viscosity, ϵ_a.

$$\epsilon(x) = L(x)U(x) + \epsilon_a \tag{73}$$

$L(x)$ and $U(x)$ are taken to be proportional to the wake width b and the velocity difference across the wake shear layer. The length and with scale are determined by:

$$L(x)U(x) = k_1 b(V_\infty - u_c(x)) \tag{74}$$

where u_c is the mean averaged velocity in the axial direction in free flow. The expression $(V_\infty - u_c(x)$ is the velocity deficit at the center line of the wake. From [16], the constant k_1 was empirically found to be $k_1 = 0.015$.
The pressure gradients of the wake are neglected and thus the model is not valid just behind the rotor. Therefore the boundary conditions at this model was given by Ainsley at 2D. It is given by a Gaussian velocity profile with the input of initial velocity deficit $D_M = V_\infty - u_c(x)$ and wake with b:

$$1 - \frac{V}{V_\infty} = D_M exp\left[-3.56\left(\frac{r}{b}\right)^2\right] \tag{75}$$

The velocity deficit and the wake width has been shown by empirical data that it may be determined by the following equations:

$$D_M = C_T - 0.05 - (16C_T - 0.5)A/1000 \tag{76a}$$

$$b = \frac{3.56C_T}{8D_M(1 - 0.5)D_M} \tag{76b}$$

where A is the area of the wind turbine. Figure 17 shows the wake development.

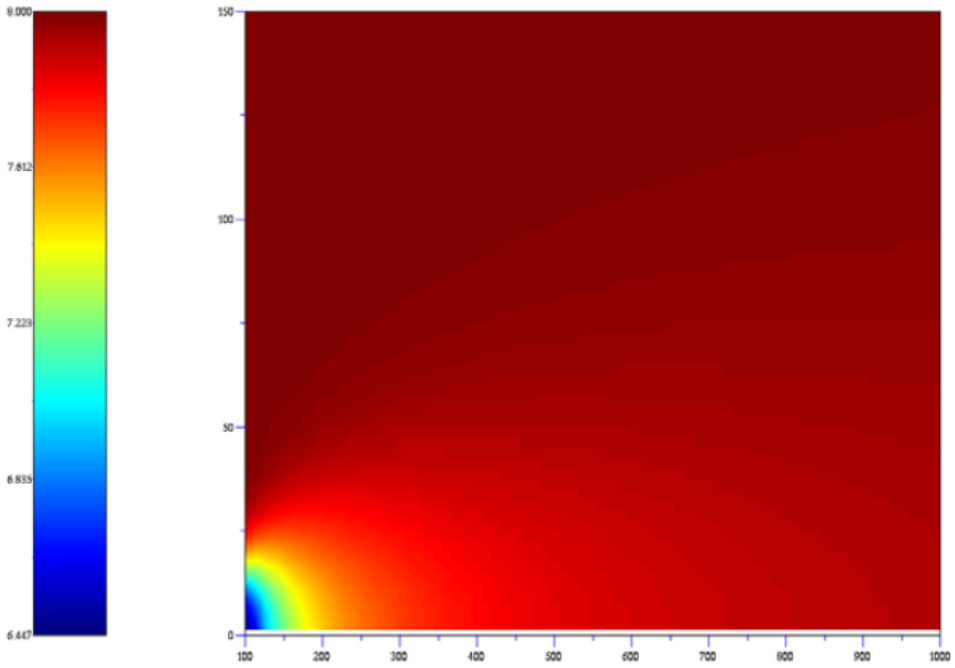

Figure 17: Wake development from the Ainlie wake model, source: [16]

5.8 WAKEFARM

The model developed by ECN is called WAKEFARM and is based on a modification of the UPMWAKE model developed by the Universidad Polytecnica de Madrid. This model is based on the 3D parabolized Navier-Stokes equations. The model is divided in a near and a far wake, the far wake are modelled with a k-ϵ turbulence model. The parabolisation of the Navier-Stokes equations a commonly accepted technique to reduce the calculational time of the wake models, it is only valid in the far wake. The near wake is modelled by using momentum theory together with rough empirical corrections.
The WAKEFARM method consists of a chain of 4 distinct models: 1) for the free stream wind speed, 2) the rotor, 3) the near wake and 4) the far wake.

The turbulent process in the far wake are modelled with the 3D RANS equations, these include the continuity equations, 3 momentum equations in three directions and the energy equation for adiabatic temperature. The equations contain the unknown kinematic eddy viscosity which is assumed to proportional to $\frac{k^2}{\epsilon}$, ϵ is the dissipation rate of turbulent kinetic energy, and the kinetic energy is k. The equations are closed with an additional transport equation for k and an equation for ϵ, see [3] for more details. The mean wind speed in three directions is then calculated.
A simplification is made, which is to neglect the axial pressure gradient in the equations. This simplification is only justified at some distance behind the turbine in the far wake. This simplification enables the parabolisation of the model and also reduces the calculational effort considerably. This is also the main reason for why the separate modelling for the near and far wake. The far wake is initialized 2.25D downstream of the rotor. The near wake is usually excluded from the wake modelling and replaced with a empirical velocity profile such to generate an initial condition to the far wake[3].

5.9 Turbulence

The turbulence in wakes are higher than in the free wind, the turbines that operate in such conditions is thus subjected to increased mechanical stress. The turbulence arise from 3 main sources[16]:

1) Orography induced turbulence, i,e. flow over hills and mountains.
2) Roughness induced turbulence, i.e. flow generated by objects within the landscape.
3) Turbine generated turbulence, i.e. turbulence in the wake of the turbines.

The turbulence intensity is important when calculating the design, lifetime and fatigue on the wind turbines. The turbulence intensity is defined as the ratio between the standard deviation of the wind speed σ_u and the 10-minute mean wind speed, U_{10}. It is "tradition" when dealing with wind turbine wakes to relate the 10-minute mean wind speed to the free stream wind velocity V_∞.

$$I_T = \frac{\sigma_u}{U_{10}} \tag{77}$$

The added turbulence in the wake may be calculated using different wake or turbulence models. There are many different models and they differ in detail level, accuracy and computational efficiency. The simplest are typically simple engineering models where the most advanced are computational fluid dynamic models which has the lowest computational efficiency.
Since most wake models include turbulence in their description, the turbulence model chosen may then affect the reduced wind speed. This may in return also change the power output, therefore, care should be given when choosing a suitable turbulence model. The Park model which is used in later sections doesn't use turbulence as input.

5.9.1 Danish Recommendation

The Danish Recommendation from 1992 specifies that the total turbulence intensity is calculated as[16]:

$$I_{total} = \sqrt{I_{amb}^2 + I_w^2} \tag{78}$$

where I_{amb} is the ambient turbulence, I_w is the turbulence added from the wake and is specified by:

$$I_w = \beta_v \beta_l 0.15 \tag{79}$$

where the parameters β_v and β_l is taking the mean wind speed and the distance between the turbines into account, respectively. β_v and β_l may be obtained as seen in figure 18 and 19.

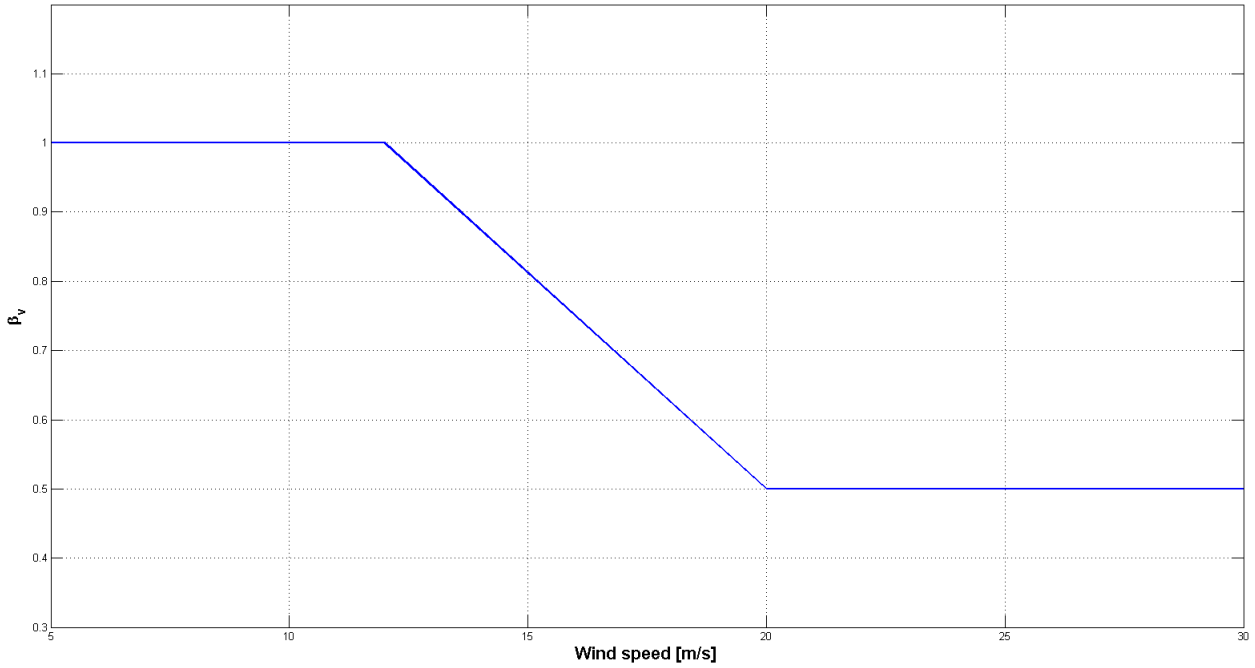

Figure 18: The factor taking the mean wind speed into account

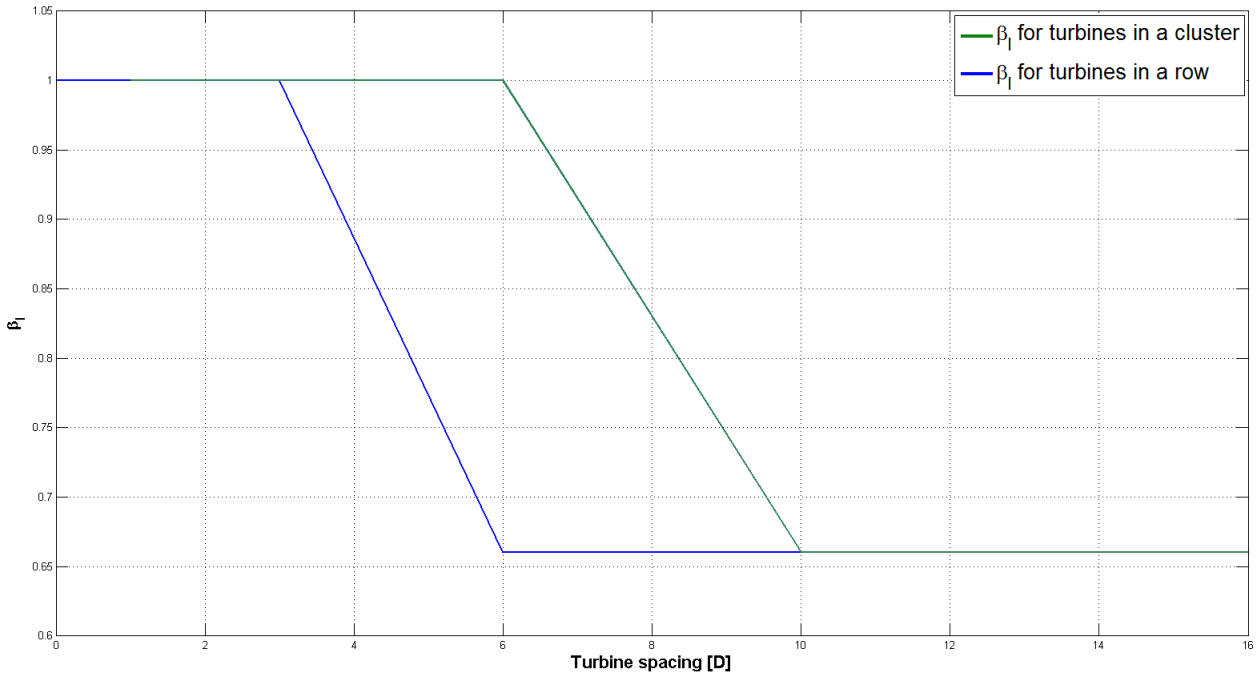

Figure 19: The factor taking the distance between the turbines into account

5.9.2 Larsen turbulence model

Larsen made his turbulence model based on the assumptions that the surface and wake shear is the only mechanisms that contribute to the generation of turbulence. The turbulence added intensity behind the turbine for spacings larger than 2D downstream is given by:

$$I_w = 0.29 S^{-1/3} \sqrt{1 - \sqrt{1 - C_T}} \tag{80}$$

where S is the spacing given in rotor diameters and C_T is the thrust coefficient[16].

5.9.3 B.Lange Turbulence Model

This turbulence model is used with the Ainslie wake model since the turbulence parameters are derived from the eddy viscosity[16].

Turbulence in the Wake

The turbulence intensity I_{total} is as we have seen, defined as the standard deviation of the wind speed process divided by the mean wind speed:

$$I_{total} = \frac{\sigma_u}{u_0} \tag{81}$$

In this model, the eddy viscosity is related to the turbulence intensity. According to Lange et al, the turbulence intensity may be calculated by using the relation with the free wind speed V_∞:

$$I_{total} = \epsilon \frac{2.4}{\kappa V_\infty z_h} \tag{82}$$

Empirical Alternative Approach

There is an alternative empirical characterization of the wake turbulence which was proposed by Quarton and Ainslie[16]. The length of the near wake is parametrized which is primarily used in relation with the Ainslie wake model. What they report, is that the empirical turbulence decay is slightly higher than other model predictions. The added turbulence intensity from the wind turbine wake is given as:

$$I_{add} = 4.8 C_T^{0.7} {I_{amb}}^{0.68} [X/X_n]^{-0.57} \tag{83}$$

where I_{add} is the added turbulence intensity from the wind turbine wake, I_{amb} is the ambient wind turbulence, X is the downstream distance and X_n is the near wake length.

While the first alternative turbulence model may only be used with the Ainslie wake model,

this empirical alternative approach may also be used with other wake models, since the near wake can be simply determined by empirical equations[16].

6 Control strategies

There are several control objectives to consider with the control of wind turbines, they are typically:

1. Maximization of the energy captured

2. Power reference tracking

3. Reduce fluctuation of the power generated

4. Alleviation of wind turbine loads

By maximizing the energy capture one increases the financial income. The power reference tracking and the reduction of fluctuations in the power generated by the turbines and the plant is important for the stability of the grid. The load alleviation is important to reduce the maintenance and increase the operational life time of the wind turbines.

6.1 The wind turbine controller

The wind turbine controller has two main tasks, to compute the pitch reference β_{ref} and the torque reference T_g^{ref}. The wind turbine is typically only using the generator speed ω_g as the feedback measurement. In region 2 wind speeds, the generator torque is often used to control the rotor speed to capture as much power as possible, the tip speed ratio should be kept at its optimum value. When the generator torque is high, the rotor will slow down and if the torque is low, the rotor accelerates. The difference between the rotor torque T_r and the generator torque is what controls the speed of the rotor. The wind turbine controller operation principle can be seen in figure 20.

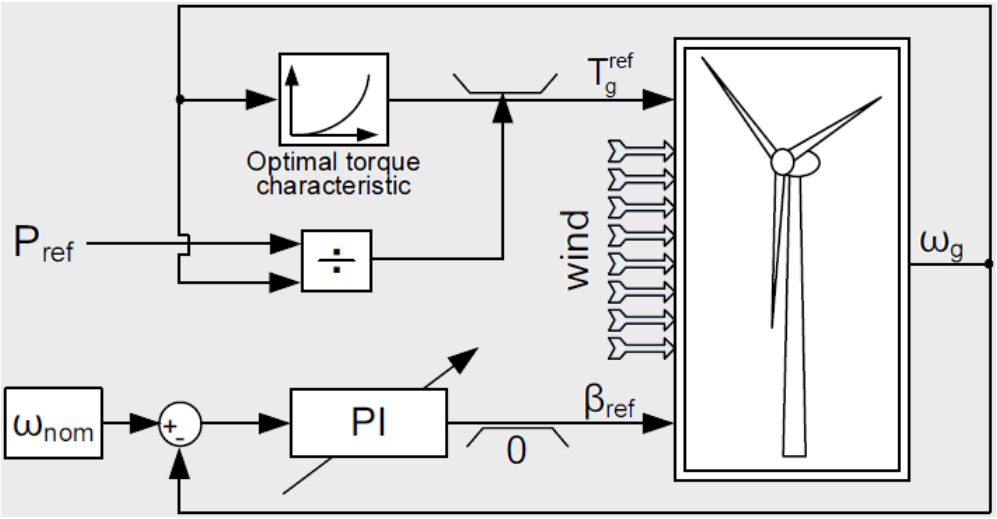

Figure 20: The wind turbine controller principle, source [7]

There are two control loops, one to set the pitch angle reference ω_g and one for the generator torque reference T_g^{ref}. If the available power is less than P_{ref}, the optimal torque characteristic part is active, this maximizes the power capture of the wind turbine. One should notice, that when the control setting is for maximum power generation, the power reference does not influence the turbine operation.

When the available power is above the power reference, P_{ref} becomes active and together with ω_g determine T_g^{ref}. Because of the high wind speed, the torque exceeds the generator torque reference, the second control loop is then activated[7].

6.2 Control of wind farms

There are two different ways for arranging the control of wind farms. The first is where each of the wind turbines are considered as isolated units, the second is where the wind farm is considered as single plant.

6.2.1 Individual turbine control

The control strategy where each wind turbine in the wind farm is considered as a single independent unit. In the literature, several strategies for set-point control of individual wind turbines are considered.

6.2.2 Collective turbine control

This control strategy, where all the turbines are considered as a group is based on multivariable control techniques. The reason for collective wind farm control systems, is to coordinate and aggregate aerodynamic, structural and electrical aspects of wind energy across wind

farms. From studies which were carried out in the USA, it was concluded that if the wind-power penetration exceeds 5% of a utility's capacity, modified power system unit and control strategies are required[30]. It is then clear that it is necessary to incorporate coordinated collective wind farm control systems in large wind farms of today, and in the future. Obviously, the goal of the wind farm control is to smooth power fluctuations and reference power tracking, maximisation of energy capture and load reduction are also important. One approach would be to design a controller based on model predictive control (MPC). This will handle interactions between the turbines and operational constraints in a optimal manner. Based on these predictions, set-points to each individual wind turbine is given. Section 6.2.4 will first give a brief overview of the MPC basics and then section 6.3 will present a control strategy based on MPC, which is proposed in [7].

6.2.3 Wind farm control strategies used today

There are many different control strategies applied to current wind farms around the world, however, it has not been easy to find any documentation about this. From the information I have gathered from a person in the Norwegian wind industry, it seems that the individual turbine control strategy is the most common.

6.2.4 MPC, basics

The controller based on Model Predictive Control uses a multivariable process model to predict future behaviour. It uses mathematical programming to optimize future performance and also handles constraints on inputs(manipulated variables(MV)) and states(controlled variables(CV)). This technique is today used for advanced process control, where the number of other areas of application are rapidly increasing.

The MPC optimization criterion may be given in the following formulation[31]:

$$J = \sum_{k=1}^{N} (Z_{k+1} - Z_{k+1}^{ref})^T Q (Z_{k+1} - Z_{k+1}^{ref}) + (U_k - U_k^{ref})^T R (U_k - U_k^{ref}) \ st. \tag{84a}$$

$$\text{Model constraints: } x_{k+1} = f_k(x_k, u_k) \tag{84b}$$

$$z_k = h_{k+1}(x_{k+1}, u_{k+1}) \tag{84c}$$

$$\text{CV constraints: } Z_{min} \leq Z_{k+1} \leq Z_{max} \tag{84d}$$

$$\text{MV constraints: } U_{min} \leq U_k \leq U_{max} \tag{84e}$$

The plant dynamics are described by a process model, which may take any required mathematical form. Process input(MV) and output(CV) constraints are included in the problem formulations and thus being handled in an optimal way.

This objective function can be seen as a QP problem. At time instant k, solve the QP to obtain an optimal and feasible input sequence. Put the first input from the optimal input sequence to the process, iterate one step and repeat the optimization. The MPC principle can be see in figure 21

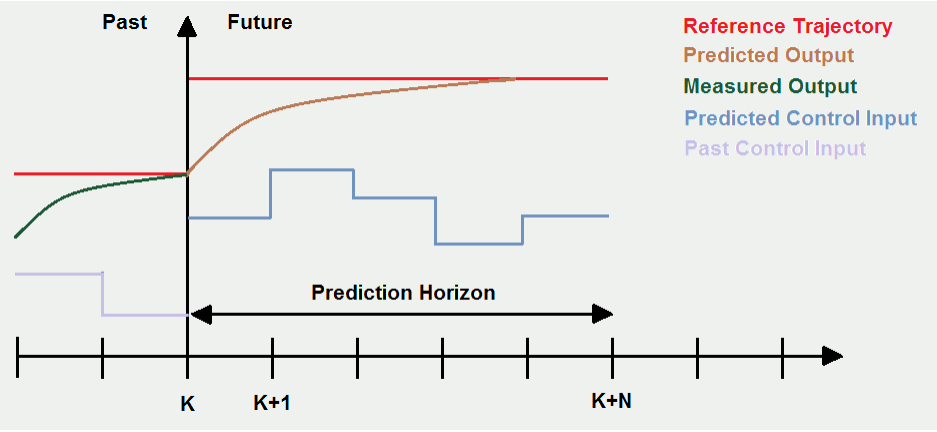

Figure 21: The MPC principle

6.2.5 Feasability and stability

To solve the MPC problem, a solution to the optimization problem must be found. However, if no feasible solutions exists, one may relax the constraints to induce feasibility to the problem. One way to relax the constraints are to soften them, that is to include a linear or quadratic penalty in the problem formulation. How the constraints are relaxed depends on the process. Some processes tolerate small values outside the constraints without breaking any safety regulations, in such cases penalty functions may be used. Physical constraints may not be softened, for example the constraints imposed by actuators.

A quadratic penalty implies that if the optimal solution is on the constraints, a small violation is allowed. One may also implement linear penalties where all violations are penalized equally the same.

6.2.6 MPC tuning

The tuning parameters are N, Q and R, where N is the prediction horizon where the future performance is optimized. The matrices Q and R where $Q \geq 0$ and $R > 0$ are weights on the error between the current and desired values of the CV and MV, respectively. The norm is to use diagonal matrices for Q and R.

6.2.7 Nonlinear MPC

Many systems are in general inherently nonlinear, in these cases linear models nonlinear models have to be used since linear models may be inadequate to describe the process dynamics. In the 90s, the nonlinear model predictive control has received increasing attention. This is because today's processes is operating under tighter performance specifications and with strict constraints from both environmental and safety considerations. These demands is often only met when the nonlinearities and constraints are explicitly considered in the controller[36]. We cannot solve the optimization problem as a single QP problem which is the case for the linear MPC. Most NMPC problems are based on Sequential Quadratic Programming(SQP) methods. SQP is an iterative method, which is effective for nonlinear constrained optimization. It generates each step(search direction) by solving quadratic subproblems as a linear QP problem. The QP problem is given by generating a linear approximation of the constraints each step.

6.3 Coordinated power reference control

Wind farms are traditionally operated as a collection of individually controlled turbines where the goal is to maximize the single turbines power production. The problem with this method is the big fluctuations of power production from the wind farm, this is a problem which may disturb the grid operation. As mentioned in previous sections, with the increased wind penetration due to growth in wind farm size, efficiency and numbers, the requirement that a wind farm operates as a single controllable entity, instead of a collection of individually uncoordinated wind turbines is necessary. The methods and formulations described in this section is presented in [7].

For the wind farm to reliably maintain a constant level of power production, limiting the power production is important. This means that the wind farm have to produce less than the available power such that it is possible to increase(or decrease) the power output as a response to changes in the power reference. To track the power reference, the individual wind turbines need to coordinated. This is the responsibility of the wind farm controller. The controller is fed a power reference and then calculates and distributes the individual wind turbines power references. Feedback is given to the controller as the measurement from the wind farm, see figure 22.

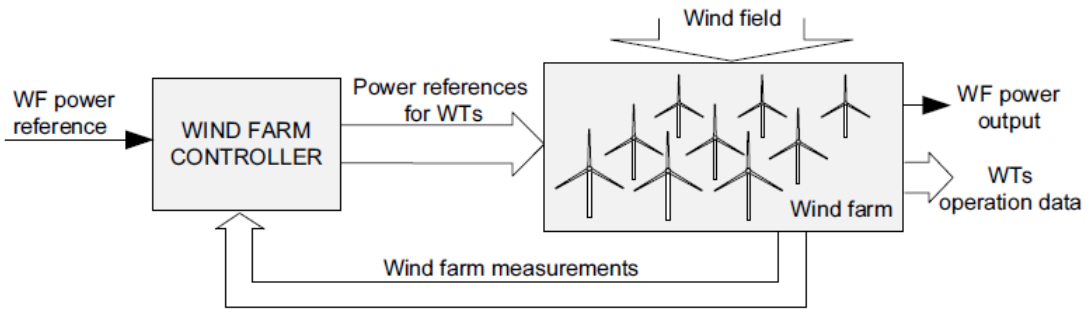

Figure 22: The control system of a wind farm. Source: [7]

6.3.1 Control objectives

There are two goals of the control objectives, the primary goal is that the wind farm electrical power output tracks the wind farm power reference. The second is the alleviation of the wind turbine loads, which refers to forces and moments on the wind turbine structure, induced by the shaft and thrust loads. The shaft loads is given by the torsional torque of the low-speed shaft. This torque is transferred through the gearbox, which is a vulnerable part of the structure. The thrust force creates material stress by the bending of the tower and blades. In the wind farm controller which has a large sampling time, we are only able to alleviate load oscillations which occurs at low frequencies. With this controller, the goal is not to hold the power output constant where the load deviate freely with the wind, but to let the power to deviate within some defined constraints such that it is possible to reduce the load.

6.3.2 Cost function

The oscillations of the wind turbine structure is influenced by both high and low frequency components, which is contributed to by the natural oscillations from the structure and also the external excitations of the wind turbine. By reducing the low frequency components in load histories we may again reduces the excitation of the structure natural oscillations.

It is assumed that there are estimates of the wind speed at each wind turbine. An initial distribution of the individual wind turbine power reference must be given, this may by found by:

$$P_{ref}^{0} = \frac{P_{ref}^{WF}}{N_{WT}} \tag{85}$$

where P_{ref}^{WF} is the wind farm power reference and N_{WT} is the number of wind turbines. These values will determine the steady state values of the wind turbines. The cost function is given such that it penalizes the deviations from the operating points and is given as:

$$J(P_{ref}(t), F_T(t), T_{shaft}(t)) = r(P_e(t) - P_{ref}^{0})^2 + q(T_{shaft}(t) - T_{shaft}^{0})^2 + q_d\left(\frac{dF_T(t)}{dt}\right)^2 \tag{86}$$

where r, q and q_d are the tuning parameters. P_e is the actual produced power, T_{shaft} denotes the low-frequency shaft torque, T_{shaft}^{0} is the steady state shaft torque, and F_T is the thrust force. The last term of the cost function is given to penalize the derivation of the trust force such that it prevents the drifting of the power reference due to fluctuations in the wind speed - the steady state thrust force is dependent on the wind speed. The values of the tuning parameters decide if the controller tracks the power or the load or a mix between the two objectives.

6.3.3 Wind farm model for MPC

The controller is to be designed as an on-line Model Predictive Controller, where the sampling time is set to 1 second. It is important that the model captures the needed dynamics of the fluctuation in wind speed and the load measures. Figure 23 describes the interface of the model. There are two inputs to the model, the wind speed v, which acts as a disturbance, and the power reference P_{ref}, which is the control input. There are three outputs, the actual electrical power P_e and the two load measures, the low-frequency low-speed shaft torsional torque T_{shaft} and the thrust force F_T.

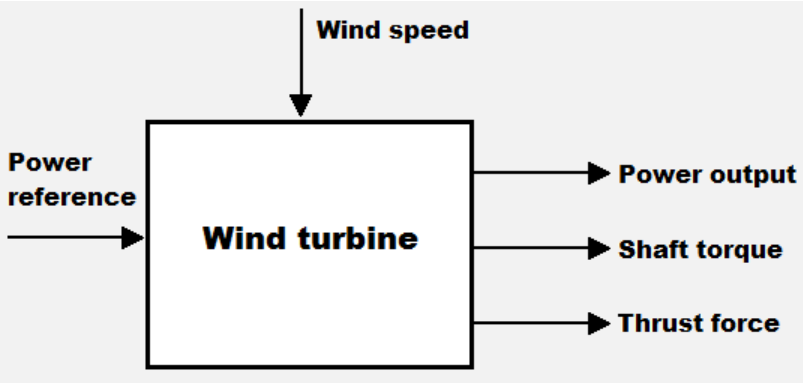

Figure 23: Model interface

The dynamic wind turbine model is found by linearization of the three equations 14, 15 and 16 which describe wind turbine dynamics. Fast dynamics are ignored such that the wind turbine transmission system may be given as a system with lumped inertia:

$$\frac{d\omega_r}{dt} = \frac{1}{J_r + i^2 J_g}(T_r(t) - iT_g(t)) \tag{87a}$$

$$\omega_g(t) = i \cdot \omega_r(t) \tag{87b}$$

where ω_g and i is the generator speed and the gear ratio, respectively. The low-speed shaft is twisted by the torque T_{shaft} and is given by:

$$T_{shaft}(t) = i^2 \cdot \frac{J_g}{J_r + i^2 J_g} T_r(t) + i \cdot \frac{J_r}{J_r + i^2 \cdot J_g} T_g(t) \tag{88}$$

where J_r is the rotor inertia and J_g is the generator inertia. Disregarding the dynamics of the electrical system, the generator model is:

$$P_e(t) = \mu T_g(t) \omega_g(t) \tag{89}$$

The pitch servo system is disregarded. This system has significant inertia, and is considered in the controller design. More detail about the simplifications may be found in [7]. The model is described in the state space form:

$$\begin{aligned} \dot{x} &= Ax + Bu + B_d d \\ y &= Cx + Du + D_d d \end{aligned} \tag{90}$$

where the vectors x, u, d, and y are the states, inputs, disturbances and outputs, respectively. Given as vectors:

$$x = \begin{bmatrix} \beta \\ \omega_r \\ \omega_g^{filt} \end{bmatrix}, \quad u = \begin{bmatrix} P_{ref} \end{bmatrix}, \quad d = \begin{bmatrix} v \end{bmatrix}, \quad y = \begin{bmatrix} F_T \\ T_{shaft} \end{bmatrix} \tag{91}$$

the state space matrices are given as:

$$A = \begin{bmatrix} 0 & -\frac{K_p^0 i}{T_\omega} & \frac{K_P^0 - K_I^0 T_\omega}{T_\omega} \\ \frac{K_{\beta T_r}}{J} & \frac{1}{J}\left(K_{\omega T_r} + \frac{P_{ref}^0 i}{\mu \Omega_g^{0\,2}}\right) & 0 \\ 0 & \frac{i}{T_\omega} & -\frac{1}{T_\omega} \end{bmatrix} \tag{92a}$$

$$B = \begin{bmatrix} 0 \\ -\frac{1}{J}\frac{1}{\mu \Omega_g^0} \\ 0 \end{bmatrix}, \quad B_d = \begin{bmatrix} 0 \\ \frac{1}{J} K_{vT_r} \\ 0 \end{bmatrix} \tag{92b}$$

$$C = \begin{bmatrix} K_{\beta F_T} & K_{\omega F_T} & 0 \\ \frac{i^2 J_g K_{\beta T_r}}{J} & \frac{i}{J}\left(i J_g K_{\omega T_r} - \frac{i J_r P_{ref}^0}{\mu \Omega_g^{0\,2}}\right) & 0 \end{bmatrix} \tag{92c}$$

$$D = \begin{bmatrix} 0 \\ \frac{1}{\mu \Omega_g^0} \end{bmatrix}, \quad D_d = \begin{bmatrix} K_{vF_T} \\ i^2 \frac{J_g}{J} K_{vT_r} \end{bmatrix}, \tag{92d}$$

where P_{ref}^0 is the power reference, β^0 and Ω_g^0 are the pitch angle and generator speed at the operating point, respectively. K_P^0 are the proportional gain and K_I^0 are the integral gain of the speed tracking PI controller at a given operating point. The coefficients $K_{\beta T_r}$, $K_{\omega T_r}$, $K_v T_r$, $K_{\beta F_T}$, $K_{\omega T_T}$, $K_v F_T$ are obtained from the first-order Taylor approximation the expressions 14 and 16 at a given operating point.

The wind farm controller is assumed to be a discrete controller with one second sampling time, the given state space model and the cost function are discretized where the control problem is in [7] defined as a Constrained Finite-Time Optimal Control problem:

$$\min_U = U' \mathcal{R} U + Y' \mathcal{Q} Y + Y_d' \mathcal{Q}_d Y_d \tag{93a}$$

$$\text{subject to} \begin{cases} \mathcal{Y} = \mathcal{C} x_0 + \mathcal{D}_u U + \mathcal{D}_d D \\ \mathcal{E}_U U \leq \mathcal{F}_U \end{cases} \tag{93b}$$

where the initial state is x_0, N is the prediction horizon. U is the optimization variable, D is the vector of predicted disturbances, Y is the vector of predicted outputs and Y_d is the vector of predicted output differences. The constraint which is most important for this control design are for the power reference:

$$P_{min} \leq P_{ref} \leq P_{max} \tag{94}$$

where P_{min} and P_{max} is the minimal and maximum power reference. The weight matrices are defined in accordance to 86:

$$\mathcal{R} = \text{diag}(R, ..., R), \mathcal{R} = \mathcal{R}' \succ 0 \tag{95}$$

which is the control weight matrix, the output weight matrix is given as:

$$\mathcal{Q} = \text{diag}\left(\begin{bmatrix} 0 & 0 \\ 0 & Q \end{bmatrix}, ..., \begin{bmatrix} 0 & 0 \\ 0 & Q \end{bmatrix} \right),\ \mathcal{Q} = \mathcal{Q}' \succeq 0 \tag{96}$$

and the output difference weight matrix is:

$$\mathcal{Q}_d = \text{diag}\left(\begin{bmatrix} Q_d & 0 \\ 0 & 0 \end{bmatrix}, ..., \begin{bmatrix} Q_d & 0 \\ 0 & 0 \end{bmatrix} \right), \mathcal{Q}_d = \mathcal{Q}_d' \succeq 0 \tag{97}$$

results of simulation is given in [7] where different tuning strategies are tested and it is concluded that wind farms may benefit from coordinated wind turbine control where it is achieved a reduction in loads while the operating conditions still holds.

6.4 Energy maximization - Operation planning

There are many parameters that decide the utilization of the wind power, the distance between the turbines, optimal geographical placing and integration in the electrical power system to name a few. With regard to maximizing the energy yield, the optimal layout and wake effects are important aspects. For an optimal wind farm layout, each wind turbine needs the sufficient down and crosswind spacing. This is because of the turbulences and wind speed deficits from the wakes will reduce the energy yield. The suitable geographical areas for wind farms are scarce, and therefore there will be a constraint on how large the spacing between the turbines may be.

The layout of a wind farm is typically built to optimize for the statistically most common wind direction. The wind direction will always fluctuate, and therefore the rotors won't be perfectly aligned towards the wind for maximum energy extraction unless yaw control is implemented. However, this maximization will only be true for the single turbine. On the other hand, by considering the wind in the prevailing wind direction, by intentionally inducing a small change in the yaw direction, the wake will be rotated and spread in the direction that is perpendicular to the rotation plane. The first wind turbines power output will be reduced because of this, but since the rotated wake won't fully shadow the downwind turbine, it will be able to extract more power due to increased wind speed. This yaw effect for the prevailing wind direction is studied in [32]. Since the direction of the wind changes, so does the optimal yaw values and ideally, one would use a lookup table for these in a real yaw control implementation. The results found in [32] shows that the maximal power output is found at a yaw angle which equals to 14°. This is because there is no wake shadowing at the downwind turbines. This result is quite obvious because the trade off which is based on the loss of power due to the difference of the wind direction and the rotational direction of the rotor, is only the cosine function to this angle, which is very low at angles as low as 14°.

When there are no more downwind turbine power extraction gains due to no wake shadowing, the loss from the difference in wind speed direction to the direction of the rotor will halt any further improvements. To implement this solution (yaw angle of 14°) in practice would be problematic, this is due to the increased structural load. A more realistic solution would probably be in the range of 5 - 8°, tests and load/cost analysis is needed for any conclusion about the acceptable maximum yaw angle. It is important to note that the optimal yaw angle found in [32] is only valid for the downwind turbine spacing used in the experiment. By increasing the downwind spacing, the optimal angle would be lower, and thus the structural loads. These are among many other variables to consider when planing the construction of wind farms.

P_sum_Y [%]		Yaw Angle of WT1, Y1 [°]																	
		0	1	2	3	4	5	6	7	8	9	10	11	12	13	14	15	16	17
Yaw Angle of WT2, Y2 [°]	0	0,0	-0,1	-0,3	-0,3	-0,1	1,2	1,6	2,0	2,6	3,4	3,5	6,2	8,5	13,1	14,9	14,4	13,8	13,3
	1	0,0	-0,1	-0,3	-0,4	-0,1	1,1	1,5	2,0	2,6	3,3	3,5	6,2	8,4	13,1	14,9	14,4	13,8	13,2
	2	-0,1	-0,2	-0,4	-0,5	-0,2	1,0	1,4	1,9	2,5	3,2	3,4	6,0	8,3	12,9	14,7	14,2	13,6	13,1
	3	0,0	-0,1	-0,3	-0,3	-0,1	1,2	1,5	2,0	2,6	3,3	3,5	6,1	8,3	12,9	14,7	14,1	13,6	13,0
	4	0,6	0,5	0,3	0,2	0,5	0,8	2,0	2,5	3,0	3,8	3,9	6,5	8,7	13,1	14,8	14,2	13,7	13,1
	5	1,2	1,2	1,0	0,9	1,2	1,5	2,6	3,1	3,6	4,3	4,4	5,9	9,0	12,5	14,9	14,4	13,8	13,2
	6	2,0	1,9	1,7	1,7	1,9	2,2	2,6	3,7	4,2	4,9	5,0	6,5	9,4	12,8	15,0	14,5	13,9	13,4
	7	2,9	2,8	2,6	2,5	2,8	3,0	3,4	4,5	5,0	5,6	5,7	7,1	9,9	13,1	15,2	14,7	14,1	13,5
	8	3,9	3,8	3,6	3,5	3,7	4,0	4,3	4,7	5,8	6,4	6,5	7,8	10,5	13,6	15,4	14,9	14,3	13,7
	9	5,0	5,0	4,8	4,7	4,9	5,1	5,4	5,8	6,8	7,4	7,4	8,7	11,1	14,1	15,7	15,2	14,6	14,0
	10	6,4	6,4	6,2	6,1	6,3	6,5	6,8	7,1	7,5	8,5	8,6	9,7	12,0	14,8	15,6	15,1	14,6	14,0
	11	8,2	8,1	7,9	7,9	8,0	8,2	8,5	8,7	9,1	10,0	10,0	11,1	12,6	15,7	16,4	15,9	15,3	14,7
	12	10,5	10,4	10,0	9,9	10,3	10,5	10,7	10,9	11,2	11,6	11,9	12,9	14,3	17,0	17,5	17,0	16,4	15,8
	13	13,9	13,9	13,7	13,6	13,7	13,9	14,1	14,2	14,5	14,8	14,8	15,7	16,8	19,0	19,3	18,8	18,3	17,7
	14	15,7	15,6	15,5	15,4	15,5	15,6	15,7	15,8	16,0	16,3	16,3	17,0	18,0	**19,9**	**20,1**	19,6	19,1	18,5
	15	15,3	15,2	15,1	15,0	15,1	15,2	15,3	15,4	15,6	15,9	15,8	16,5	17,6	19,5	19,6	19,1	18,5	18,0
	16	14,8	14,8	14,7	14,5	14,6	14,7	14,8	15,0	15,1	15,4	15,4	16,1	17,1	19,1	19,1	18,5	18,0	17,4
	17	14,4	14,3	14,2	14,1	14,1	14,2	14,4	14,5	14,7	14,9	14,9	15,6	16,6	18,6	18,5	18,0	17,4	16,8

Figure 24: Percentage of difference in total energy production with yaw change, source: [32]

Remember the strategy discussed in section 5.1 where the upwind turbine power extraction is lower than the downwind turbines such that the total energy production is increased. A possible way to further increase the energy maximization would be to combine this strategy with the optimal yaw effects - this will be tested by simulation in the next section.

7 Cases of study and simulation

In this section, we will study the effects of the optimal yaw planing combined with the effects of a reduction of the power output from the upwind wind turbines, where the front turbine reduces its power output the most. The simulation is divided into 3 parts:

1. In the first part, we will see how the wake affects the power output where each turbine operates at the same power coefficient C_p.
2. In the second part, we will do the same as in part 1, but include the yaw effects.
3. In the third part, we will combine the setup in part two with the effects of upwind turbine power output reduction.

The results gathered from each of the three parts will then be compared to find the possible improvement of such a setup.

7.1 Wind wake model and setup

The wake model used in this simulation is the Jensen(Park) wake model. One problem which may lead to errors in the calculation of the wake shadowing effects are the simplification which leads to the sharp edges of the wake. Even with this "on and off" boundary characteristic, it's has been shown that compared to the more realistic wake models such as the Ainslie model, the old Jensen(Park) model gave the least difference from the actual wake loss[33]. Shadowing effects from yaw rotation was not included in this wake model comparison.

7.1.1 Choice and influence of the WFC

It was shown in [33] that the N.O. Jensen(Park) model gave the most accurate results when calculating the wake losses. To get such good results, it is very important to choose the correct value of the Wake Decay Coefficient(WDC), given as k. The WDC has a great influence on the calculation and the result of the wake speed deficit. The WDC is not only affecting the wind speed deficit, but also at the same time the rate of expansion of the wake. This can be seen from the equation for the wind speed deficit:

$$\delta V_{01} = V_\infty(1 - \sqrt{1 - C_T}) \left(\frac{D_0}{D_0 + 2kX_{01}} \right)^2 \frac{A_{overlap}}{A_1} \tag{98}$$

where the rate of expansion is given as:

$$kX_{01} \tag{99}$$

Because this model doesn't include a turbulence model, it is quite obvious that this constant is closely linked to the ambient turbulence of the wind. When we have low turbulence, higher

wake loss occur which also means that we need to set a low value of WDC. The ambient turbulence is also to a large degree a function of the terrain roughness, different weather conditions also affects the ambient turbulence. Therefore, even though the model is relatively simple, it is still important to analyse the surrounding geographical and meteorological conditions before using this model. Suitable values for the WDC is about 0.03-0.075 depending on the roughness of the terrain[33]. In this simulation, the value of k is set to 0.05.

7.2 Wind farm setup

The simulation will consist of three wind turbines that are placed in a row. The turbines have rated power of 2 MW with a diameter of 80 meters. The downwind spacing is set to 300 meters which equals to $3.75D_0$. The three turbines in this simulation has the coordinates (0,0), (0,300), (0,600), see figure 25.

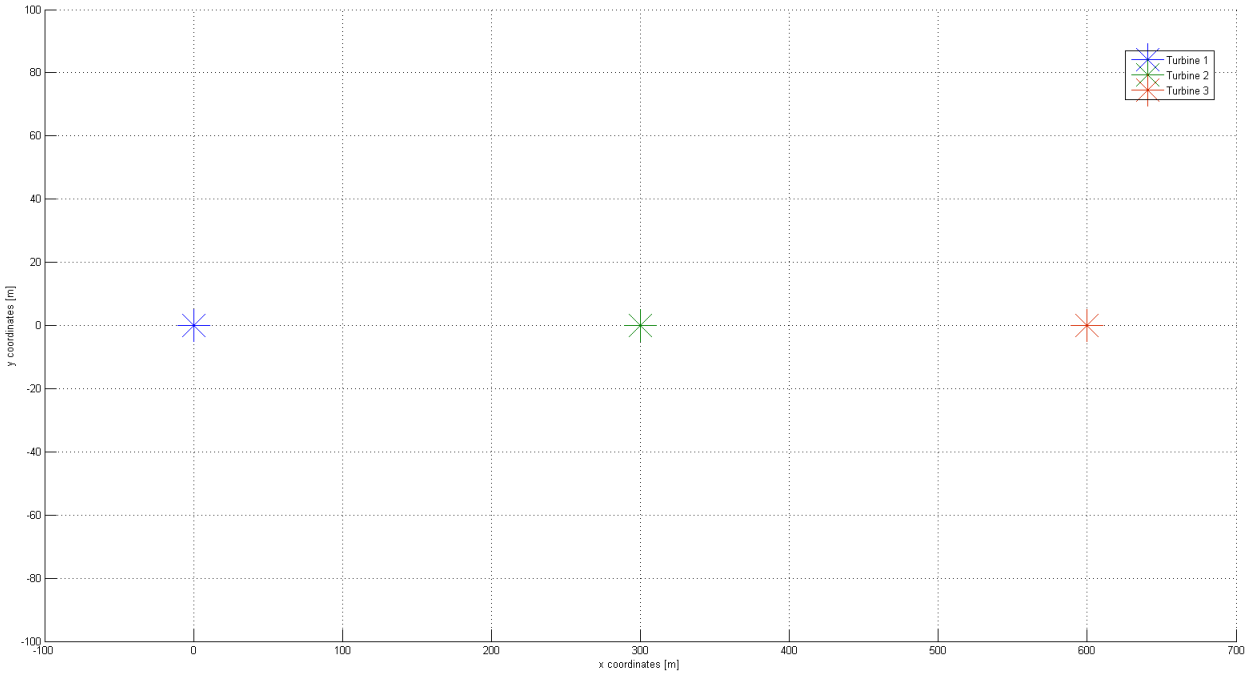

Figure 25: Coordinates of the three turbines used in the simulation

The rated wind speed which will be constant for the duration of the simulation, is set to $15\frac{m}{s}$. The wind direction is assumed to be constant which is the prevailing wind direction. The power coefficient C_P is set to 0.4. The most important values used in this simulation are shown in table 1 which may be found at the end of this section. Three wind turbines is used in this simulation because of the fact that array losses are low (less than 10%) under typical inflow conditions when the downwind spacing are 8-10 or more rotor diameters, see section 6. Since the downwind spacing is $3.75D_0$, the distance to turbine 4 from turbine 1 would be $11.25D_0$, the wake interaction would then be negligible.

7.2.1 Simulation - Part 1

In this part we will test the power production generated by each turbine. The downwind turbine 2 is completely in the wake of turbine 1 and turbine 3 is in a combination of the wake of turbine 1 and 2, details of how this is calculated is given in section 5.5.2. The power coefficient C_P is the same for all the three turbines and is set to 0.4. The power generated by each turbine can be seen in figure 26.

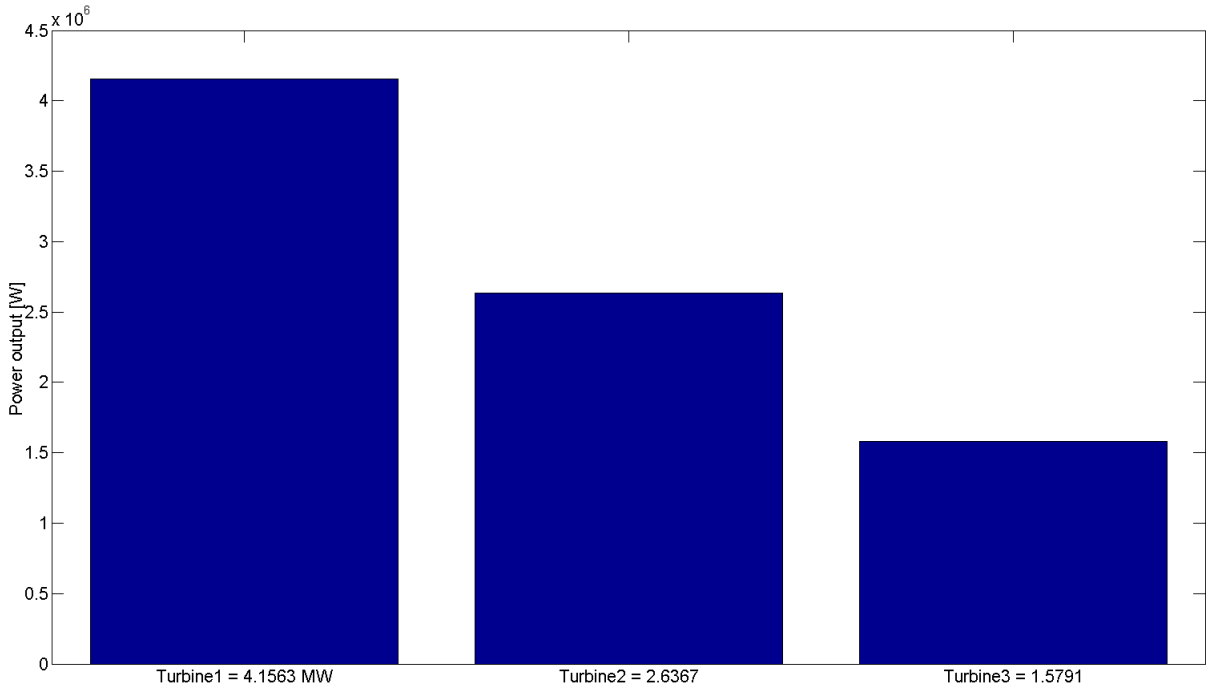

Figure 26: Power output from each individual turbine.

We can see from figure 26 that the downwind turbines produce much less power than the most upwind turbine. The total power output from all the three wind turbines was $8.372MW$.

7.2.2 Simulation - Part 2

In this part of the simulation we will investigate the influence of a change in the yaw angle on the two first wind turbines, turbine 1 and turbine 2. The power coefficients is as in part 1 set to 0.4. The yaw angle is for this simulation set to 7 degrees, the result from this simulation can be seen in figure 27. The total power output where the result is compared to part 1 can be seen in figure 28. We can see that the total power production increased by 10.46% compared to part 1.

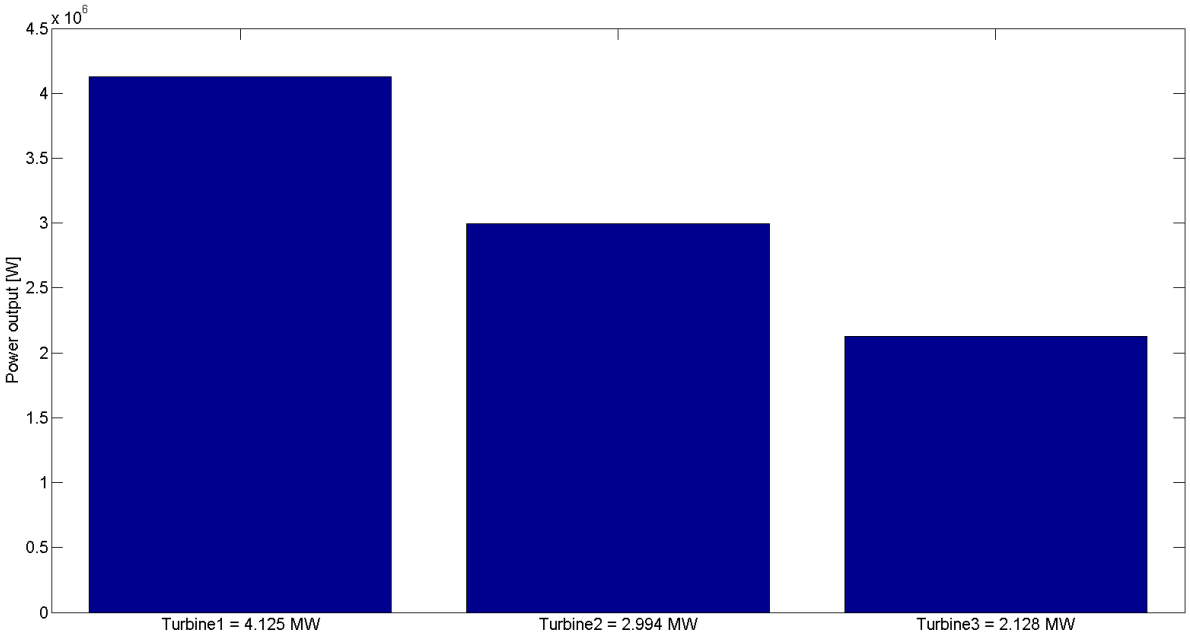

Figure 27: Power output from each individual turbine with a yaw of 7 degrees.

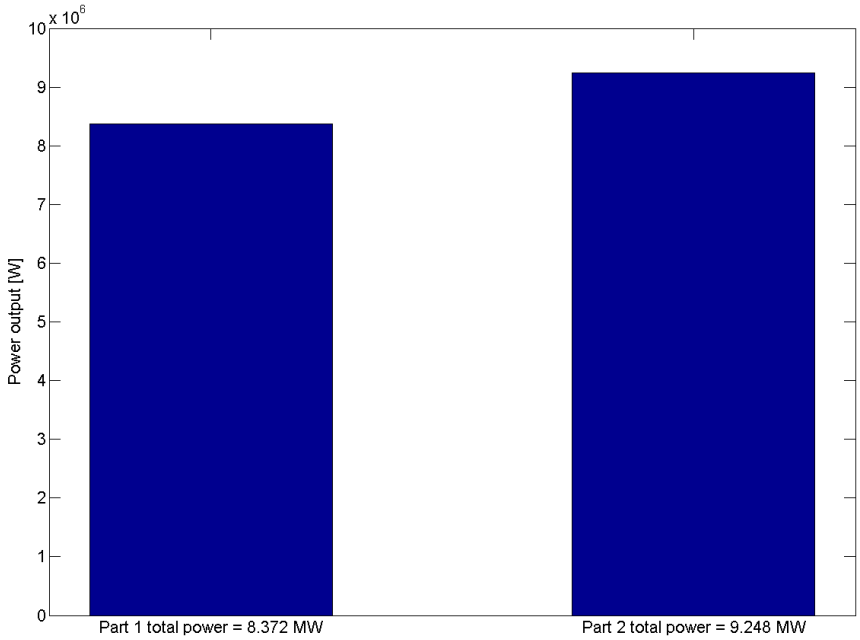

Figure 28: Total power output, comparison of the result without and with a yaw of 7 degrees.

7.2.3 Simulation - Part 3

In this part we will investigate the potential for further power output increase by reducing the upwind power extraction of the upwind turbines. The values of the individual turbines power coefficient will be changed and the the resulting power output from each case will be compared. The simulation will first be done without the yaw effect and then with the same yaw configuration as in part 2. The result for the case where no yaw is used can be seen in figure 29.

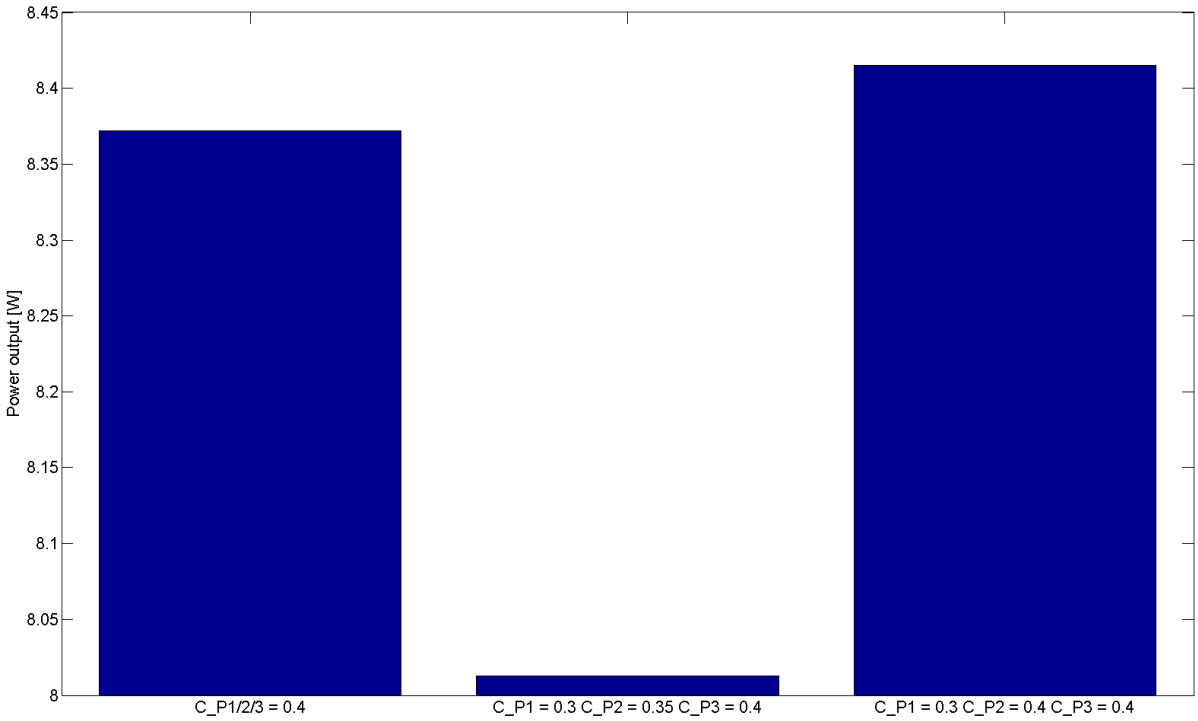

Figure 29: The total power with different values of the power coefficient on the individual turbines

we can see from the result where only the first turbine has decreased its power coefficient, that the total power production has increased by 0.51% compared to the case where the power coefficients are held constant. This result is as expected because by reducing the power extracted from the first turbine, both the downwind turbines will be able to extract power from the higher wind speeds. It was found that when the power coefficient from turbine 1 got lower than around 0.27, the total power production was reduced. The difference between a power coefficient of 0.3 and 0.27 was insignificant, thus the value of 0.3 was chosen for this experiment. The next case for testing was by using a yaw of 7° and 10°, the results can be seen in figure 30 and 31, respectively.

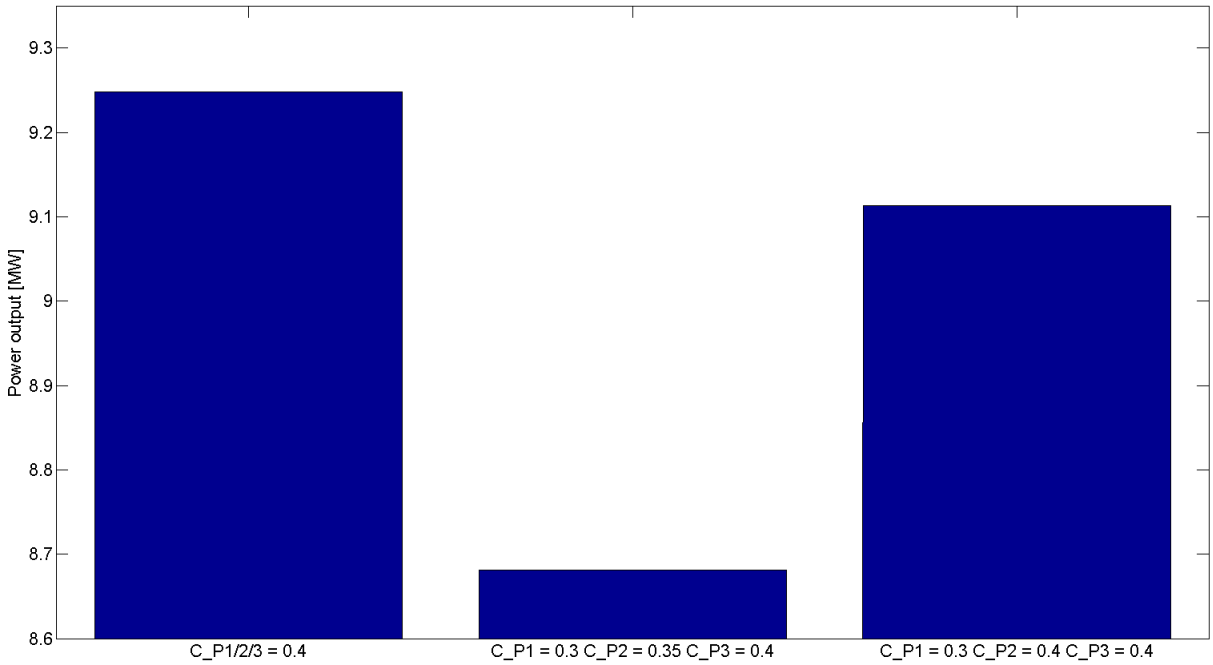

Figure 30: The total power with different values of the power coefficient on the individual turbines when yaw is set to 7 degrees

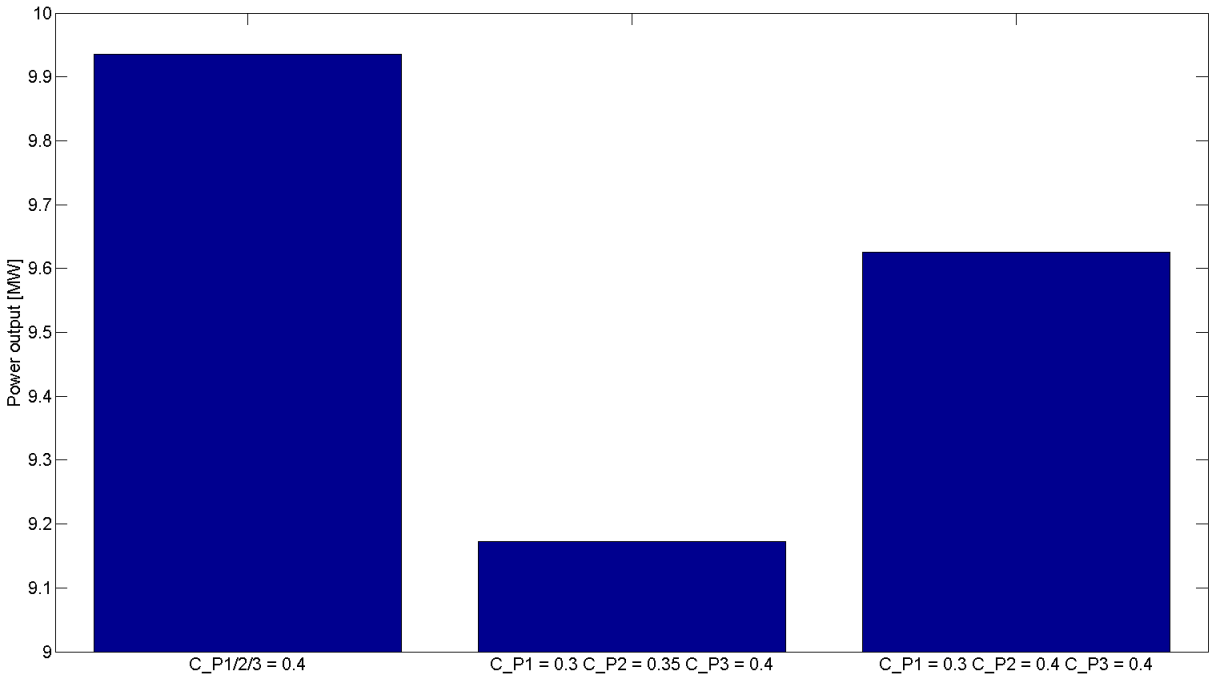

Figure 31: The total power with different values of the power coefficient on the individual turbines when yaw is set to 10 degrees

From figure 30 and 31 we can see that for the cases where the yaw is 7° and 10°, the result is now different from the case with no yaw. Instead of a power increase by 0.51%, when the yaw is rotated 7° the power is 1.45% lower than compared to the case where a constant C_P is used. When the yaw is rotated 10°, the total power is 3.12% lower.

7.3 Discussion - Simulation results

From the results from the three different simulation parts, we can see that both the yaw effect and the front turbine power reduction influence the individual turbine and the total power production. The interesting part of these simulations would be to see if a combination of the two strategies may increase the total power production - we see from the simulation results that this isn't the case. When we combine the front turbine power coefficient reduction with the yaw effect, the total power production decreases when compared to the results with the yaw effect alone. Intuitively, this may suggest that when the wake has less overlap on the downwind turbines, the positive effect from the power coefficient reduction is also reduced. The yaw effect has a much higher potential to increase the total power production than compared to the effects from the front turbine power coefficient decrease. The 7° yaw effect by it self gave a total power production increase of 10.46% while the decrease of the front turbine power coefficient gave a increase of 0.51%. We may from these results conclude that a combination of these two result in a lower total power output than the yaw effect alone.

Figure 32 and 33 shows the increase in total and individual power production, respectively. From 33, we can see that the power production of turbine 1 decreases as the yaw increases, but at the same time, the power production of turbine 2 and 3 increases. The power production decrease in turbine 1 is because of the winds angle of attack changes which reduces the power output as the cosine of the angle of attack (the yaw in our case). The output of turbine 2 and 3 increases until there is no more overlap from the rotation of the yaw, the power output then starts to decrease with further increase in yaw from the same case as with turbine 1.

The increase in the power production from the yaw control strategy was quite high. It is possible that real values would be lower, this is because of our simple model that doesn't consider all effects in its calculation.

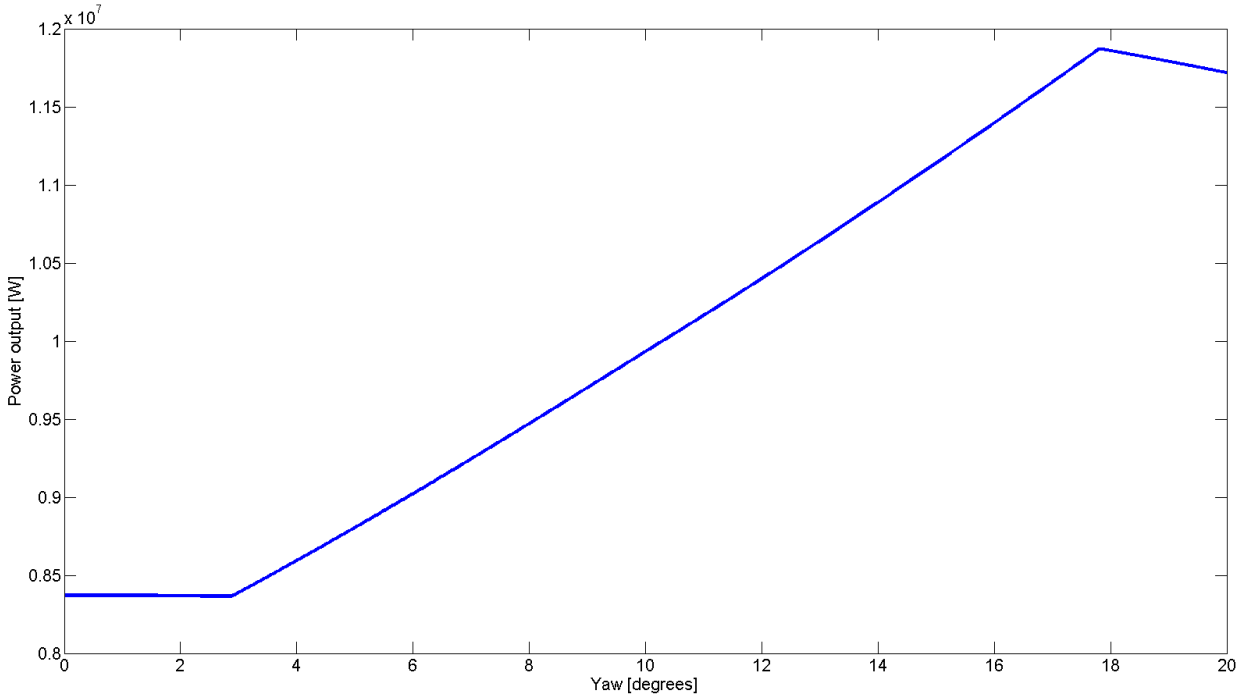

Figure 32: The total wind farm power production as a function of the yaw angle

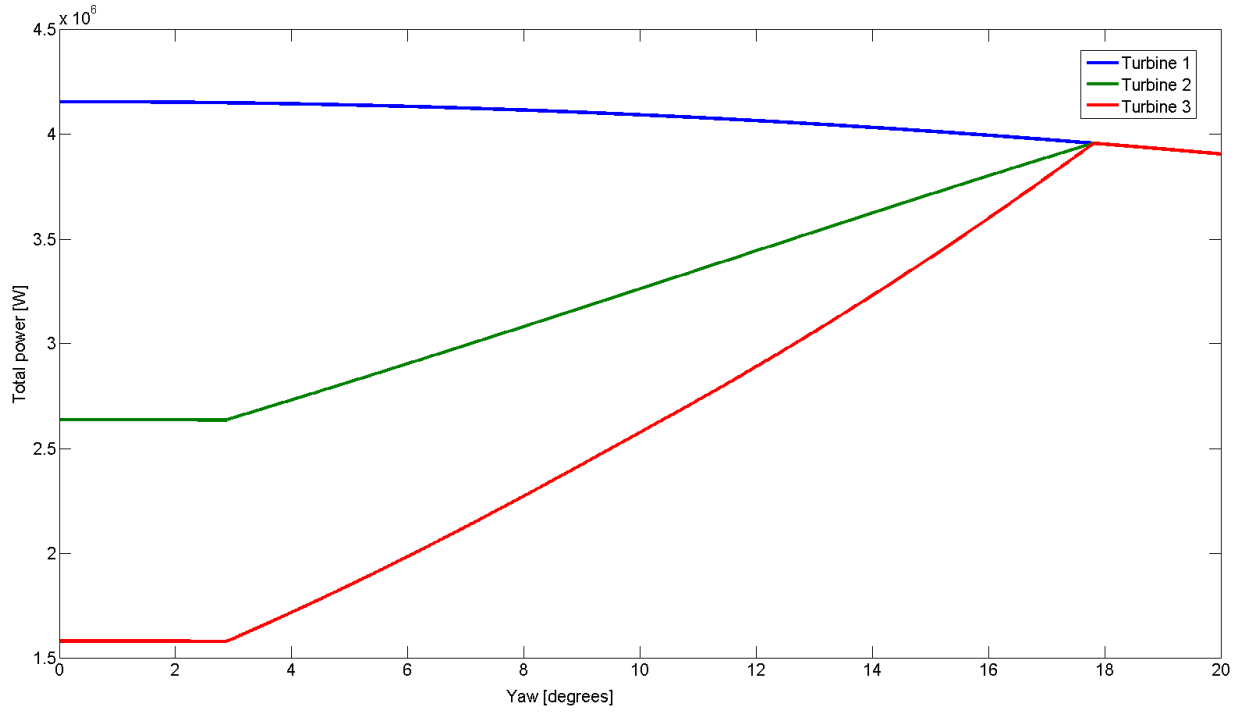

Figure 33: The individual turbine power production as a function of the yaw angle

Table 1: Simulation parameter values

Parameter	Symbol	Value
Prevailing wind speed	V_∞	15m/s
Power coefficient	C_p	0.4
Air density	ρ	1.225
Wake decay constant	k	0.05
Rotor diameter	D_0	80m

8 Discussion

As the wind energy penetration increases, it is clear that the coordination and control of the wind farm power production is very important. This is not only because of the profit from increased power production, but also to secure the grid stability and environmental benefits. While single turbines are often still treated as single power generators connected to the power grid, it seems to be inevitable that coordinated wind farm power control will become the norm. While weather fluctuations still exists, improvements in weather forecasting will minimize this uncertainty of wind power, this stability factor will further increase the value of wind power.

Wind farm planning is not a trivial task and the contributing factors to a good wind turbine site are many. The most important aspects are high wind speeds without too large seasonal fluctuations and the proximity to a grid connection. What also is becoming more and more important is the environmental impacts, this include the proximity to historical monuments and animal habitats. Probably the main issue for the developers planning onshore wind farms today is the problems connected to the proximity to people and local communities.

Other aspects with wind farms are the operation planning, such that one may maximize the energy yield. The first thing to consider when planning a new find farm is the optimal wind turbine positioning, such that wake effects are minimized and at the same time the total power output is maximized. It is not possible to find one optimization that is suited for all wind farm sites, this is because of the geographical variations which influence how the wind turbines interact. Other focuses of the wind farm operation planning are how control mechanisms may be utilized to change the mutual interaction between the wind turbines, generated by the downwind wakes. In this report, we investigated the effect from yaw control, not to direct the rotor blades perpendicular against the wind, but to rotate the wake away from the downwind turbines. The second strategy investigated, was to decrease the power coefficient in upwind turbines. We could see from the simulation results that the yaw effect had more potential to increase the total wind farm power output. The reduction of the most upwind turbine also gave a slight increase in the total power production when no yaw effect was used. The gain from this was much less than what was possible to gain from the yaw effect, when the two effects were combined, we actually got a lower increase in the total power output compared to the yaw control strategy alone.

From these results, it is clear that in the case to optimize the operation planning of a wind farm, only the yaw effect should be considered. The main problem with this kind of yaw control is the trade-off between the extra profit from the higher power output and the extra costs from the extra structural loads. There should be possible to do a cost analysis on this to find an optimal yaw angle such that the income from this exceeds the extra costs. This report assumes that the prevailing wind direction is constant, the optimal yaw angle should be found for other wind directions as well. A lookup table for the different yaw angles may then be used for different wind angles.

9 Conclusions

In this report, we have discussed the implications of higher wind energy penetration, the importance of weather forecasting along with descriptions of time series models used for wind prediction. Different wake models have been described and the mutual wake interactions among the wind turbines in a wind farm have been discussed. We have tested two strategies that can be used in wind farm operation planning to maximize the total energy production. The first strategy was to use yaw control to rotate the downwind wake away from the downwind turbines. The second strategy was to reduce the front turbines power coefficients to investigate the possibility of an increase in the energy yield. Individually, both strategies gave improvements. From the simulations, it could be seen that a yaw angle of 7° gave an increase of 10.46% compared to 0.51% from the second strategy. A combination of them gave a lower power production increase than the yaw strategy alone. Therefore, yaw control alone should be used to optimize the power production of a wind farm.

10 Appendix

The simulation part of the project was done in Simulink. A brief explanation of the blocks and subsystems will be given. The wake model implemented was the modified Park wake model, the details are described in the project report.

When we open the Simulink mdl-file, the first window that appears can be seen in figure 34.

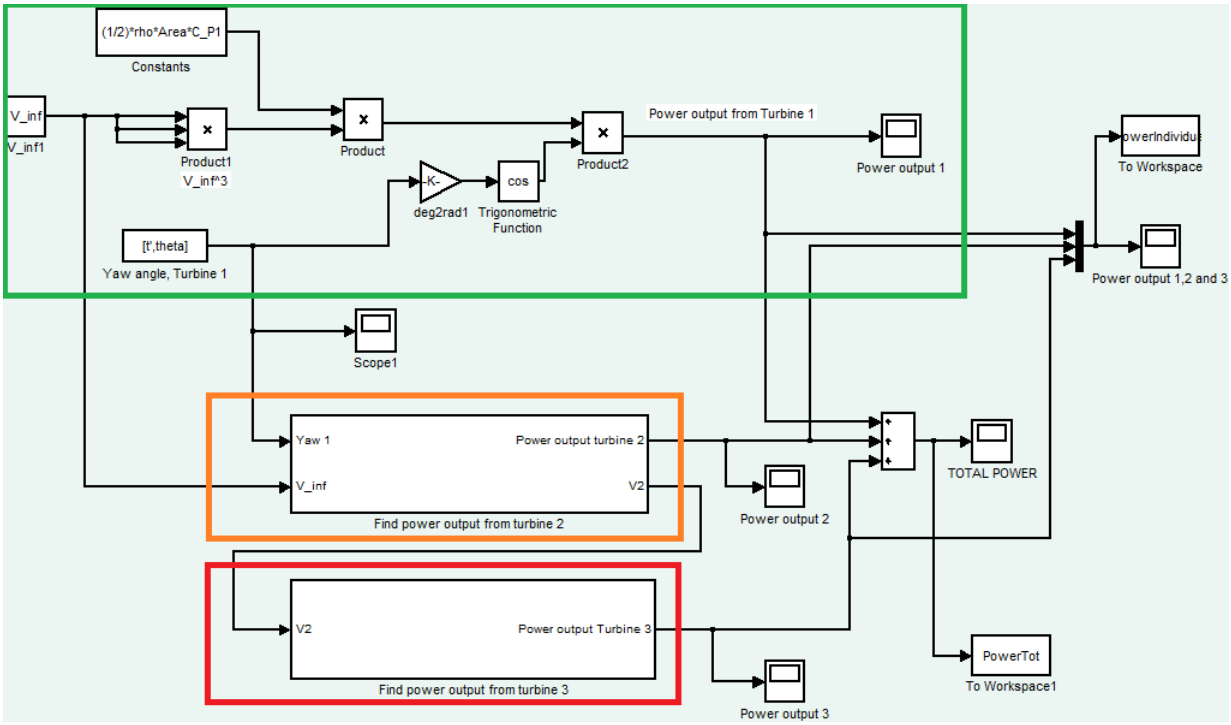

Figure 34: The main Simulink window.

GREEN: Is where the power output of the front turbine(turbine 1) is calculated. We can see that the power output is dependent on the yaw angle of the turbine. The power produced is reduced as the cosine function of the angle of attack. Since the wind direction is assumed to be constant, the angle of attack equals the turbine yaw angle.

ORANGE: Is where the power output of turbine 2 is calculated.

RED: Is where the power output of turbine 3 is calculated.

Turbine 2

Inside the "Find power output from turbine 2" block is shown in figure 35.

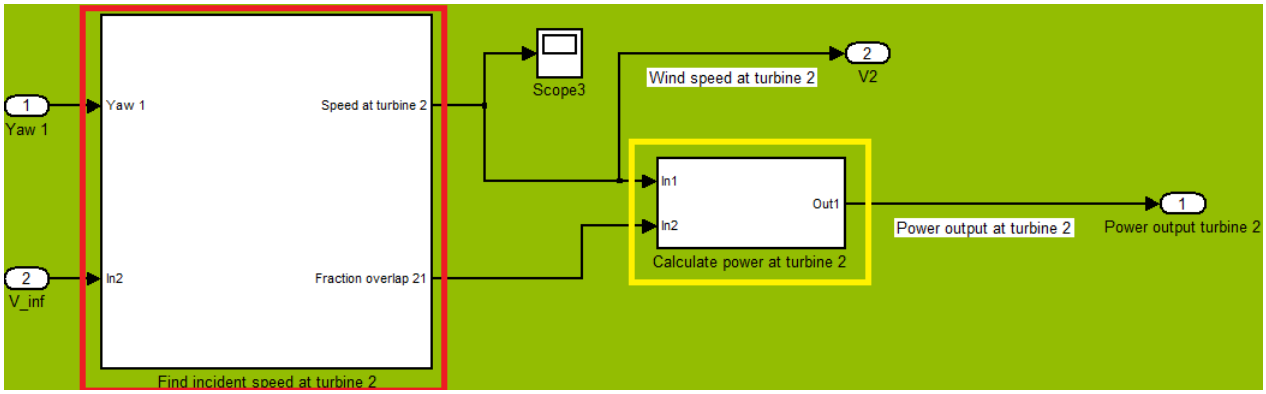

Figure 35: Power output from turbine 2.

RED: Is where we calculate the incident wind speed at turbine two. The two inputs are the free wind speed and the yaw angle at turbine 1.

YELLOW: Is where the power output of turbine 2 is calculated.

Figure 36 shows inside the ”Find incident speed at turbine 2” block, as seen in figure 35.

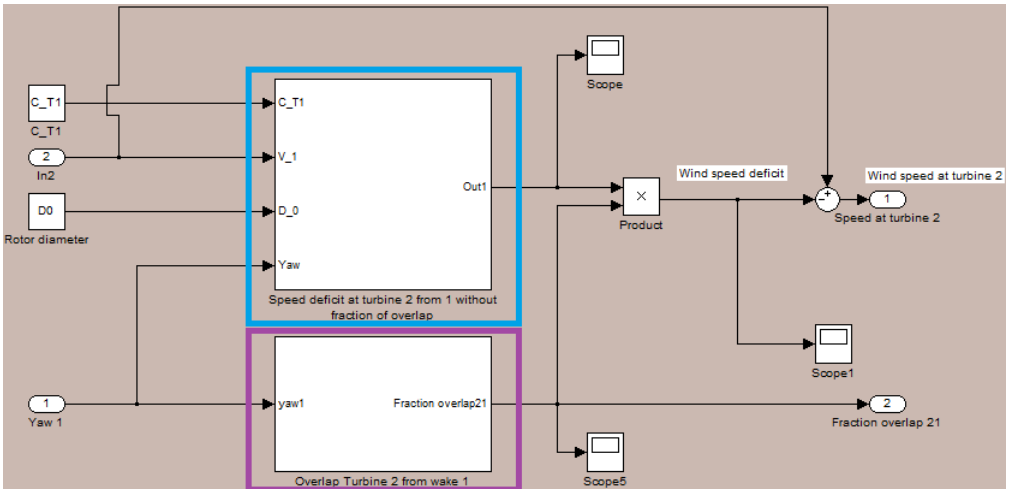

Figure 36: Shows the two blocks that calculate wind speed at turbine two, this is used to calculate the power output.

BLUE: Is where the speed deficit at turbine 2 is calculated, the inputs to this block is the thrust coefficient, the wind speed at turbine 1(which equals V_∞) and the rotor diameter.

PURPLE: Is where the fraction of wake overlap of turbine 2 is calculated.

Figure 37 shows the ”speed deficit at turbine 2” block.

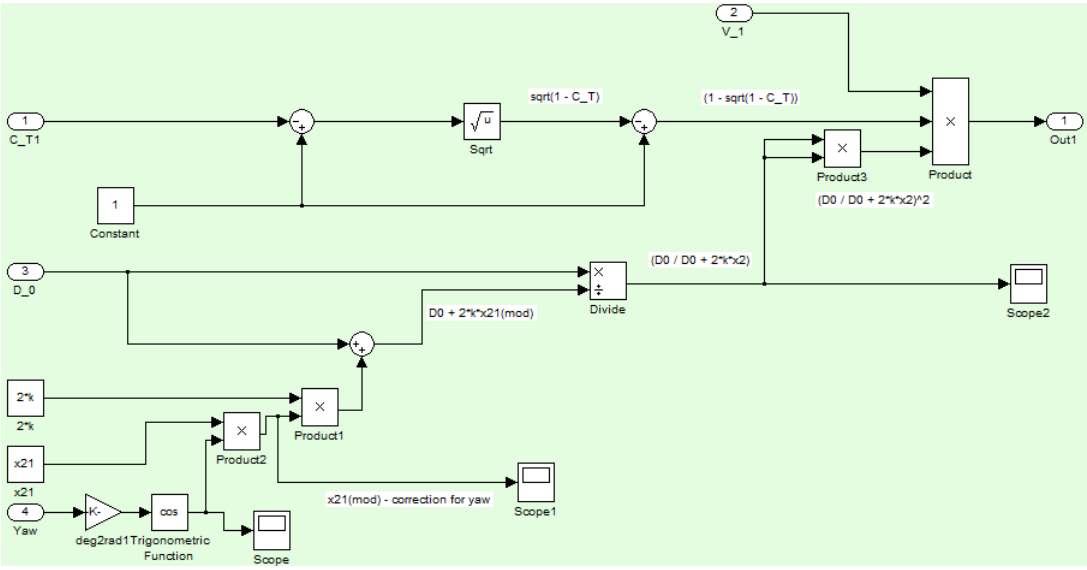

Figure 37: Shows the calculation of the wind speed deficit at turbine 2.

This is where we calculate the wind speed deficit at turbine two by the downwind wake from turbine 1. The expression for the speed deficit is:

$$\delta V_{01} = V_\infty(1 - \sqrt{1 - C_T}) \left(\frac{D_0}{D_0 + 2kX_{01}} \right)^2 \frac{A_{overlap}}{A_1} \tag{100}$$

where $\frac{A_{overlap}}{A_1}$ is calculated in the ”Overlap Turbine 2 from wake 1” block, see figure 36.

Figure 38 shows the blocks that calculate the fraction of overlap by the wake of turbine 1.

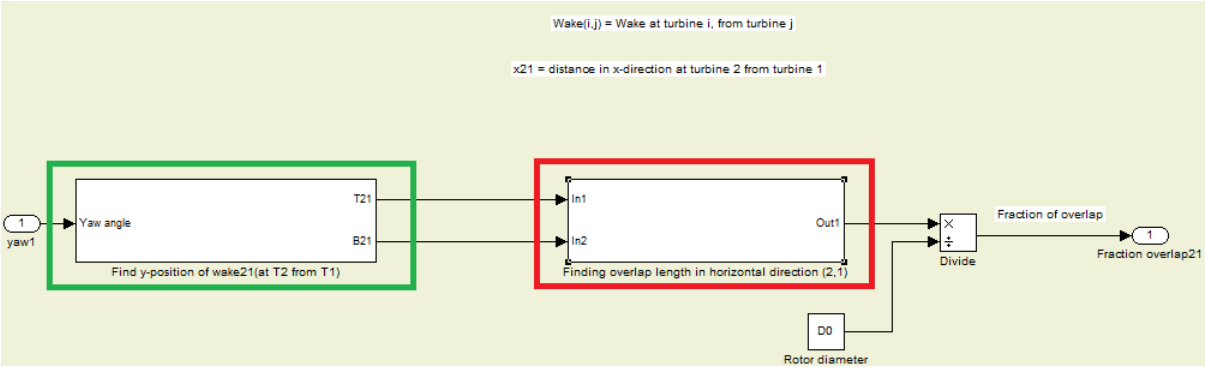

Figure 38: Shows the two blocks that calculate the fraction of overlap at turbine 2 from the wake of turbine 1.

GREEN: The purpose of this block is to find the position of the wake from turbine 1 in the x-direction where turbine 2 is located.

RED: Inside this block, the amount of overlap (in meters) is calculated with the information about the position of the wake boundaries. This result is divided by the rotor diameter to find the fraction of overlap. The modified Park wake model is used, details may be found in the project report.

Figure 38 shows the ”Find y-position of wake 21(at T2 from T1)” block, see figure 38.

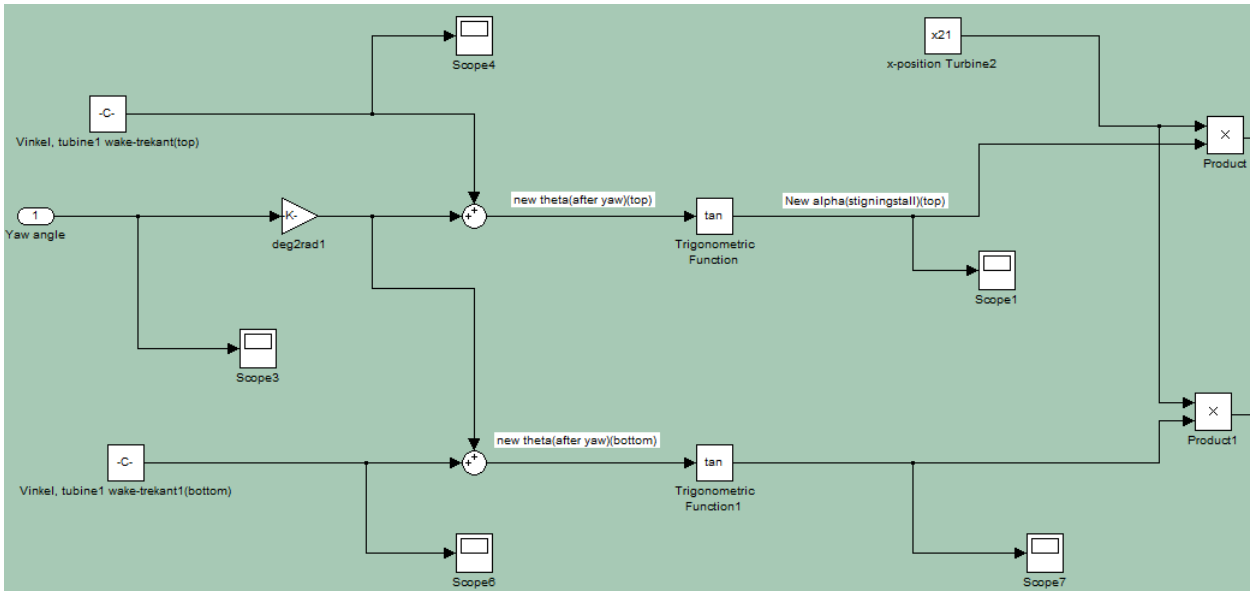

Figure 39: Inside the block where the top and bottom of the wake boundary at the x-position of turbine 2 (Part 1 - left side)

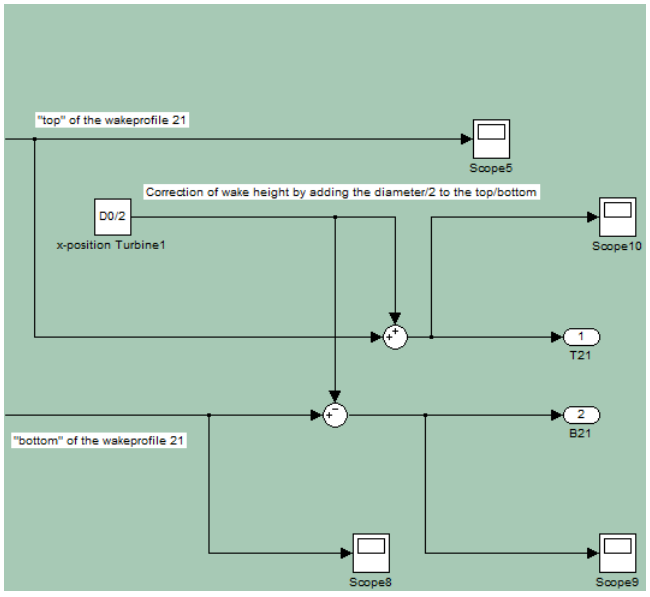

Figure 40: Inside the block where the top and bottom of the wake boundary at the x-position of turbine 2 (Part 2 - right side)

Explanation of figure 39 and 40:
The wake decay constant gives the rate at which the wake expands. We have the value of the slope when the yaw is 0. One may then find the angle of this slope, when we change the yaw, we thus add the ”original” angle of the slope with the yaw angle - then finding the new value of the slope. By knowing the distance to the downwind turbine, we may find the position of the top and bottom of the wake boundary.

Figure 41 shows the ”Finding overlap(2,1)” block, see figure 38.

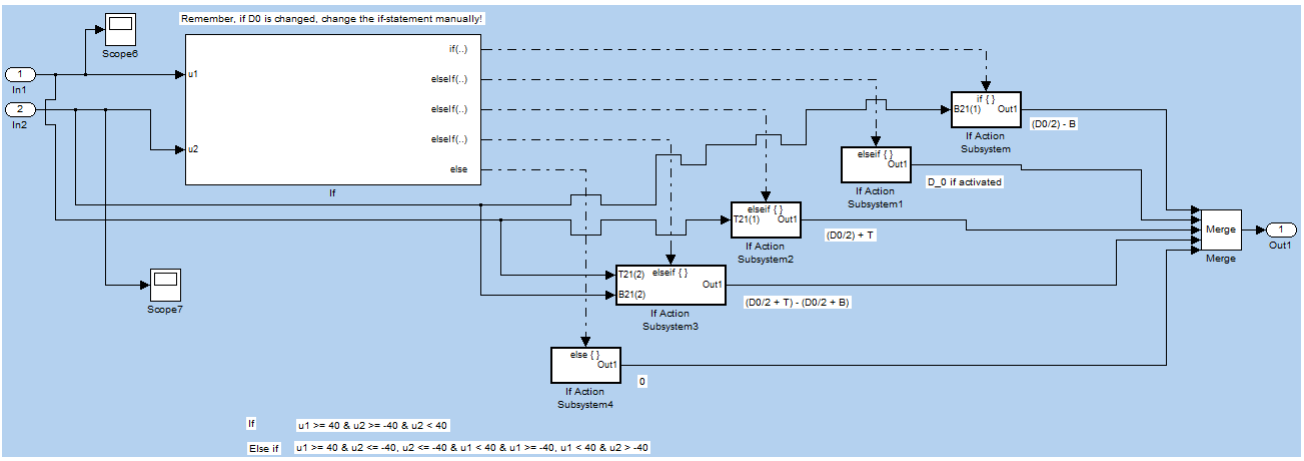

Figure 41: The overlap is found by using the if-block and if-action subsystems

The ”top” and ”bottom” of the wake boundary at the x-position of turbine 2 is compared with the top and bottom position of the rotor blades of turbine 2 by the use of if-statements. The different action subsystems calculate the amount of wake ”shadowing” in meters.

By using yaw control, the coordinates of the top and bottom of the rotor blade changes. In this calculation, however, it is assumed that no yaw is present. The potential errors caused by this should be small as long as the yaw angle is low.

Figure 42 shows the ”Calculate power at turbine 2” block, see figure 35.

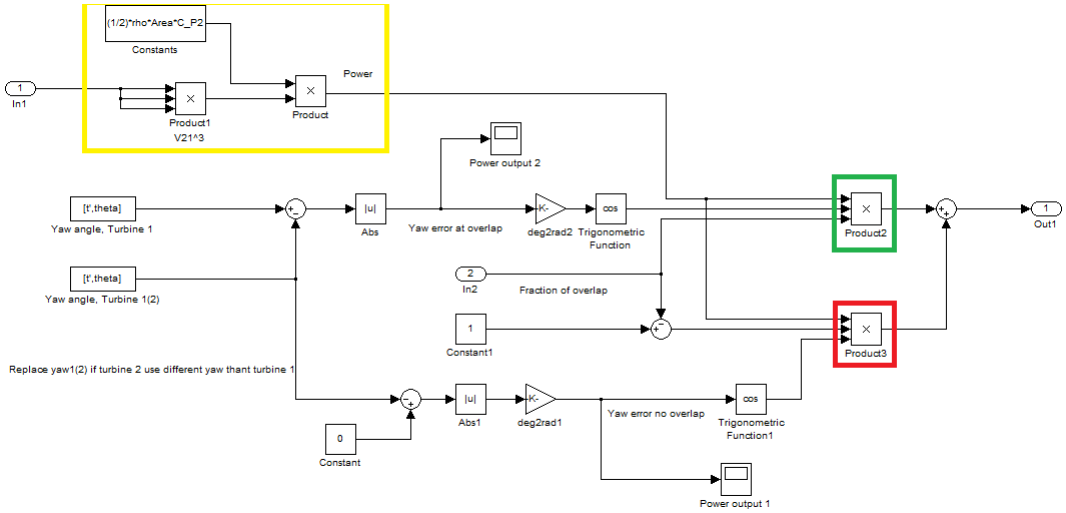

Figure 42: The calculation of the power output of turbine 2

YELLOW: This is where the power is calculated.

The Park wake model doesn't take yaw effects with the new wind angle of attack in its calculation. Therefore, to lower the turbine power production the following simplification was made. By using the fraction of overlap, we may determine which part of the turbine that is not affected by the wake. By assuming that this part is affected by the free wind stream, we may take the angle of attack into consideration, thus lowering the total output when yaw is present.

GREEN: Taking into account the wind angle of attack at the part of the rotor which is shadowed by the wake.

RED: Taking into account the wind angle of attack at the part of the rotor which is not shadowed by the wake.

Turbine 3

No detail of the implementation of turbine 3 will be given in this guide, this is because the same blocks are used, only with different x-coordinates. The multiple wake calculation is used, this is described in the project report.

11 Bibliography

[1] Kathryn E. Johnson and Naveen Thomas, "Wind farm control: addressing the aerodynamic interaction among wind turbines", 2009 American Control Conference, June 10-12, 2009.
[2] M. Magnusson, A.-S. Smedman, "Air flow behind wind turbines", Journal of Wind Engineering and Industrial Aerodynamics 80 (1999) 169 - 189.
[3] J.G. Schepers and S.P. van der Pijl, "Improved modelling of wake aerodynamics and assessment of new farm control strategies".
[4] Zhongzhou Yang, Yaoyu Li and John E. Seem, "Individual Pitch Control for Wind Turbine Load Reduction Including Wake Interaction", 2011 American Control Conference, June 29 - July 01.
[5] Sten Frandsen, "On the wind speed reduction in the center of large clusters of wind turbines", Journal of Wind Engineering and Industrial Aerodynamics, 39 (1992) 251 - 265.
[6] Rogerio G. de Almeida, Edgardo D. Castronuovo, and J.A. Pecas Lopes, "Optimum Generation Control in Wind Parks When Carrying Out System Operator Requests", IEEE Transactions on power systems, vol. 21, No. 2, May 2006.
[7] Vedrana Spudic, Mate Jelavic, Mato Boatic, "Wind Turbine Power References in Coordinated Control of Wind Farms", Automatika 52(2011) 2, 82 - 94.
[8] Vedrama Såidoc. Mato Baotic and Nedjeljko Peric, "Wind Farm Controller Design Based on Parametric Programming".
[9]European Renewable Energy Council, "20% by 2020", http://www.erec.org/fileadmin/erec_docs /Documents/Publications/Renewable_Energy_Technology_Roadmad.pdf
[10] The Minnesota Public Utilities Commission, "2006 Minnesota Wind Integration Study", November 30, 2006
[11] Michael Milligan, Pearl Donohoo, Debra Lew, Erik Ela, and Brendan Kirby, "Operating Reserves and Wind Power Integration: An Internal Comparison", NREL, October 2010.
[12] International Energy Agency, "Variability of wind power and other renewables: Management Options and Strategies".
[13] B.Sanderse, "Aerodynamics of wind turbine wakes", Litterature review.
[14] Peter J.Scubel and RIchard J.Crossley, "Wind Turbine Blade Design", University of Nottingham.
[15] Magdi Ragheb and Adam M.Ragheb, "Wind Turbines Theory - The Betz Equation and Optimal Rotor Tip Speed Ratio", University of Illinois.
[16] Morten Lybech Thøgersen, "Introduction to Wind Turbine Wake Modelling and Wake Generated Turbulence".
[17] M. Ragheb, "Control of wind turbines", 5/6/2009.
[18] Lucy Pao, "A Tutorial on the Dynamics and Control of Wind Turbines and Wind Farms", University of Colorado.
[19] Wind Energy Handbook, "http://www.gurit.com/files/documents/2_Aerodynamics.pdf".
[20] Terje Gjengedal, "TET15 Vindkraft", Statkraft SF, NTNU 2004.
[21] R.G.de Almeida and J. A. Pecas Lopes, " Participation of Doubly Fed Induction Wind Generators in System Frequency Regulation", IEEE TRANSACTIONS ON POWER SYS-

TEMS. VOL 22, NO 3, August 2007.
[22] International Energy Agency, " Variability of Wind Power and Other Renewables: Management options and strategies".
[23] Openwind Theoretical basis and validation, "http://www.awstruepower.com/wp-content /media/2011/04/OpenWindTheoryAndValidation.pdf", version 1.3.
[24] J.A. Andrawus, "Maintenance Optimisation for Wind Turbines", The Robert Gordon University, April 2008.
[25] A.M. Foley, P.G. Leahy, A. Marvuglia and E.J. McKeogh, "Current methods and advances in forecasting of wind power generation", Renewable Energy 37, 2012.
[26] R. Nayak, P.S. Patheja and A.A Waoo, "An Artificial Neural Network Model for Weather Forecasting in Bhopal", IEEE-ICAESM-2012) March 30, 31, 2012.
[27] R. Dahyot, "Time series and Applied Forecasting", Trinity College Dublin, Ireland 2012.
[28] P. Louka, G. Galanis, N. Siebert, G. Kariniotakis, "Improvements in wind speed forecasts for wind power prediction purposes using Kalman filtering", Journal of Wind Engineering and Industrial Aerodynamics 96 (2008) 2348-2362.
[29] Brown & Hwang, "Introduction to Random Signals and Applied Kalman Filtering", Third edition.
[30] Christopher J.Spurce, "Simulation and Control of Windfarms", University of Oxford, 1993.
[31] Lars Imsland, "Introduction to Model Predictive Control"
[32] N.S.Moskalenko, K. Rudion and Z.A. Styczynski, "Wind Farm Operation Planning Using Optimal Yaw Angle Pattern (OYAP), 2011 IEEE Trondheim PowerTech.
[33] T. Sørensen, M.L. Thøgersen and P. Nielsen, "Adapting and calibration of existing wake models to meet the conditions inside offshore wind farms", EMD International A/S.
[34] "Wind Turbine Power Calculations", "http://www.raeng.org.uk/education/diploma /maths/pdf/exemplars_advanced/23_wind_turbine.pdf, The Royal Academy of Engineering.
[35] "Principles of Doubly-Fed Induction Generators", http://www.labvolt.com/downloads /download/86376_F0.pdf
[36] R. Findeisen, "An Introduction to Nonlinear Model Predictive Control", University of Stuttgart.
[37] D.G. Baker, "Climate of Minnesota", University of Minnesota, 1983.
[38] "Montana wind energy atlas", Energy Division, Dept. of Natural Resources and Conservation, 1984.